Now in the 65th year

Atomically Precise Metal Clusters

Thalappil Pradeep

Institute Professor, IIT Madras

https://pradeepresearch.org/

pradeep@iitm.ac.in

Co-founder

InnoNano Research Pvt. Ltd.
InnoDI Water Technologies Pvt. Ltd.
VayuJAL Technologies Pvt. Ltd.
Aqueasy Innovations Pvt. Ltd.
Hydromaterials Pvt. Ltd.
EyeNetAqua Solutions Pvt. Ltd.
DeepSpectrum Innovations Pvt. Ltd.

Associate Editor

ACS Sustainable Resource Management

Professor-in-charge

International Centre for Clean Water

Quantum Dots – Seeds of Nanoscience

KUNGL. VETENSKAPS-AKADEMIEN
THE ROYAL SWEDISH ACADEMY OF SCIENCES

THE NOBEL PRIZE IN CHEMISTRY 2023

The Royal Swedish Academy of Sciences has decided to award the Nobel Prize in Chemistry 2023 to

©Johan Jarnestad/The Royal Swedish Academy of Sciences

Moungi G. Bawendi
Massachusetts Institute of Technology (MIT), Cambridge, MA, USA

Louis E. Brus
Columbia University, New York, NY, USA

Alexei I. Ekimov
Nanocrystals Technology Inc., New York, NY, USA

'for the discovery and synthesis of quantum dots'

How small are these 'Quantum Dots'?

A quantum dot is a crystal that often consists of just a few thousand atoms. In terms of size, it has the same relationship to a football as a football has to the size of the Earth.

Remembering pioneers

THE NOBEL PRIZE IN CHEMISTRY 2023

Michael Faraday – Divided metals

Lord Kelvin – Melting depends on size?

Richard Feynman, Nobel Prize 1965 –
Plenty of room at the bottom

Robert F. Curl, Harold W. Kroto and Richard E. Smalley Nobel Prize 1996

Andre Geim and Konstantin Novoselov, Graphene, Nobel Prize 2010

Jean Pierre Sauvage, J. Fraser Stoddart, and Bernard Lucas Feringa, Molecular machines Nobel Prize 2016

Quantum effects arise when particles shrink in size

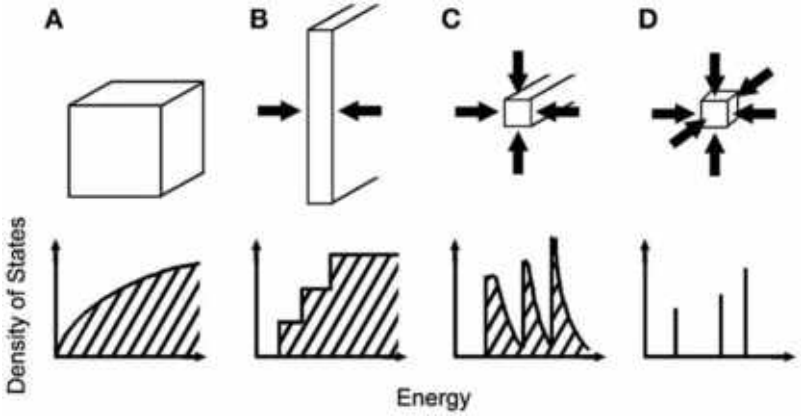

Energy levels of semiconductor crystallites with different dimensionalities.

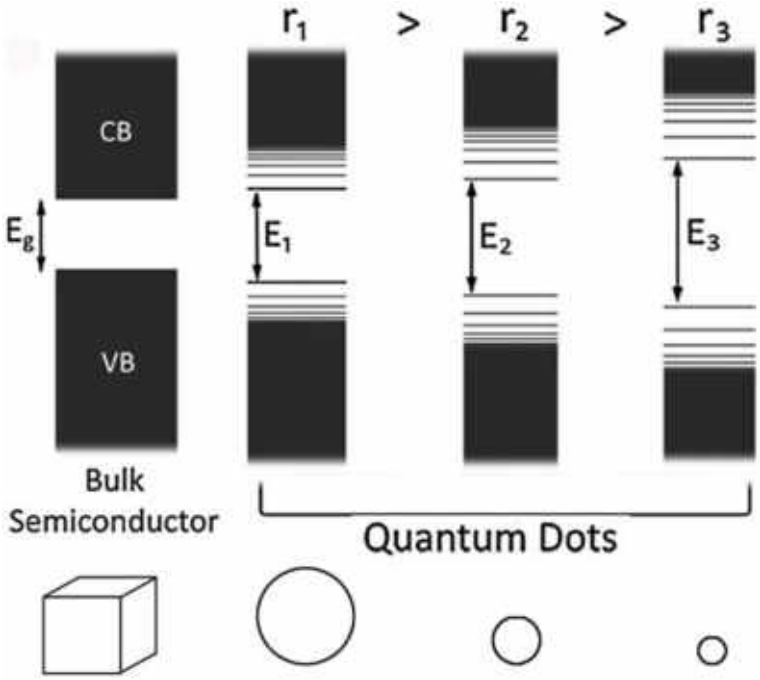

Illustration of size-dependent bandgap.

G. Dong, H. Wang, G. Chen, Q. Pan, J. Qiu, Frontiers in Materials 2015, 2.

Illustration of quantum dots

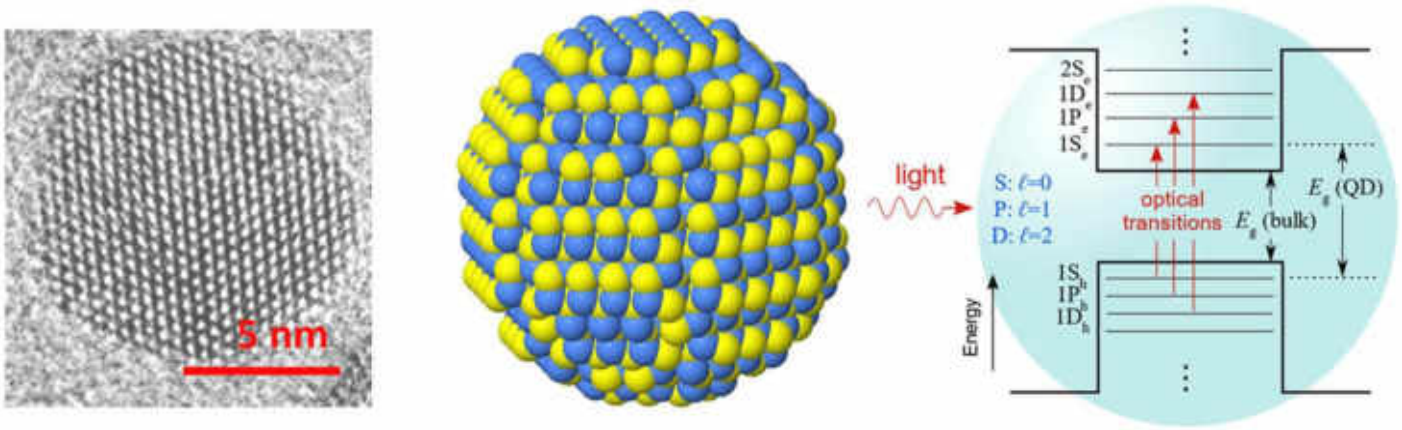

Left: transmission electron microscope image of a CdSe nanocrystal. Centre: Atomic structure of a nanocrystal. Right: Electronic states in a core-shell quantum dot, with the dot itself in the centre bracketed by a wide-bandgap shell.

A. L. Efros and L.E. Brus, ACS Nano 15, 6192 (2021).

Today, 'quantum dot' refers to a nanostructure in which quantum mechanical effects manifest themselves in the electronic structure.

- Either through quantum size effects, many-body interactions (excitonic states) or high surface-to-volume ratio such that surface states dominate the electronic structure.
- In addition to a small size comparable to the carriers' de Broglie wavelength, it is now recognized that the quantum phase coherence length (typically limited by inelastic scattering) needs to exceed the system size.

Gas phase

PRODUCTION OF LARGE SODIUM CLUSTERS (Na_x, $x \leqslant 65$) BY SEEDED BEAM EXPANSIONS

Manfred M. KAPPES, Roland W. KUNZ * and Ernst SCHUMACHER
Institute of Inorganic and Physical Chemistry, University of Bern, CH-3000 Bern 9, Switzerland

Received 10 August 1982

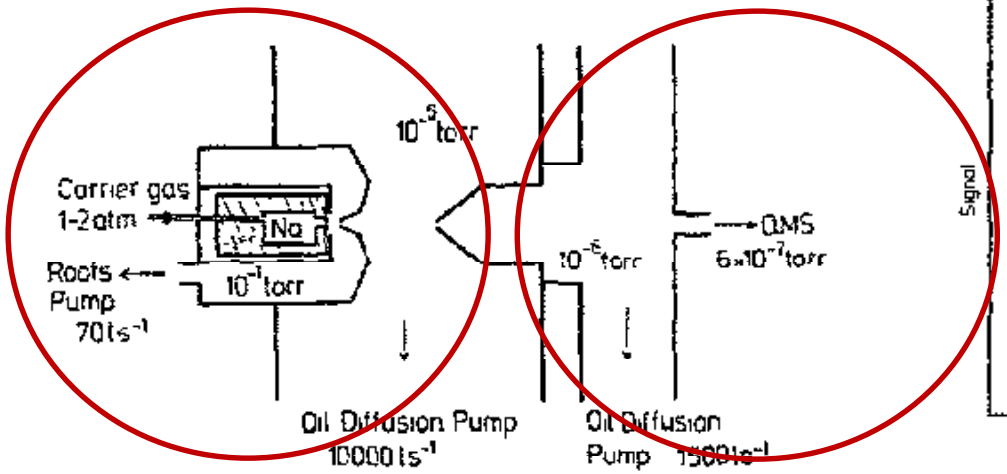

Fig. 1. Schematic of the seeded-beam apparatus.

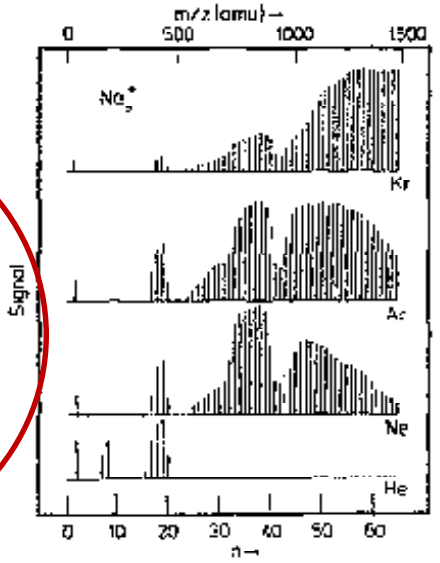

Fig. 3. Data sets showing the results of high-mass scans measured for four different backing gases. The mass spectra upon which these representations are based were obtained at a resolution ($m/\Delta m$) of 400 and a maximum signal-to-noise ratio of 20. Backing pressures were 1.3 atm for all these gases. A 1.5 mm aperture skimmer was used. With krypton, argon and neon, ions were detected up to m/z = 1495 corresponding to Na_{65}^+.

Gas phase cluster spectroscopy

Gas phase

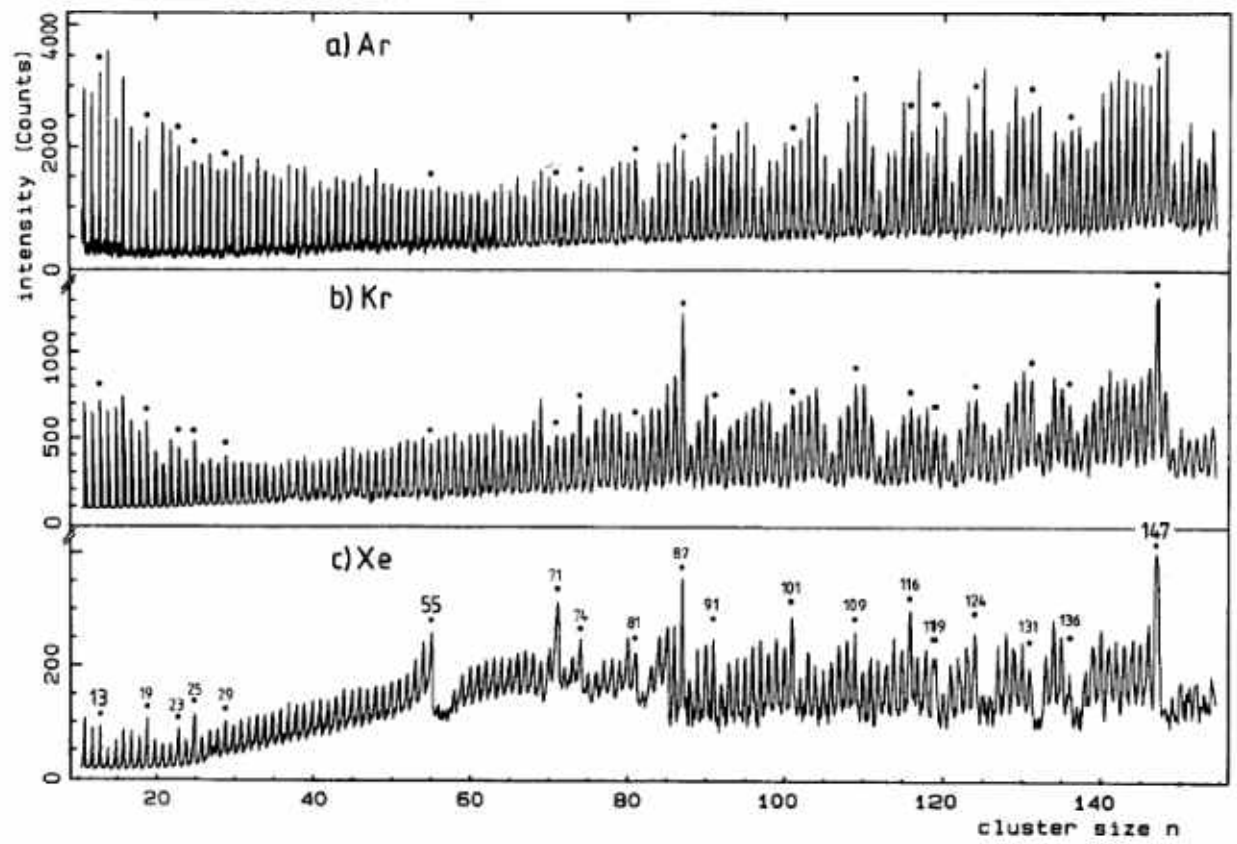

Ti_8C_{12}
Fe, Al clusters

Mass spectra of positively charged Ar, Kr, Xe clusters, W. Miehle, O. Kandler, T. Leisner, and O. Echt. (**1989**) *J. Chem. Phys.*, 91, 5940.

Gas phase

International Journal of Mass Spectrometry and Ion Processes, 74 (1986) 33–41
Elsevier Science Publishers B.V., Amsterdam – Printed in The Netherlands

MASS DISTRIBUTIONS OF NEGATIVE CLUSTER IONS OF COPPER, SILVER, AND GOLD

I. KATAKUSE, T. ICHIHARA

Department of Physics, Faculty of Science, Osaka University, Toyonaka, Osaka 560 (Japan)

Y. FUJITA, T. MATSUO, T. SAKURAI and H. MATSUDA

Institute of Physics, College of General Education, Osaka University, Toyonaka, Osaka 560 (Japan)

(First received 6 May 1986; in final form 27 August 1986)

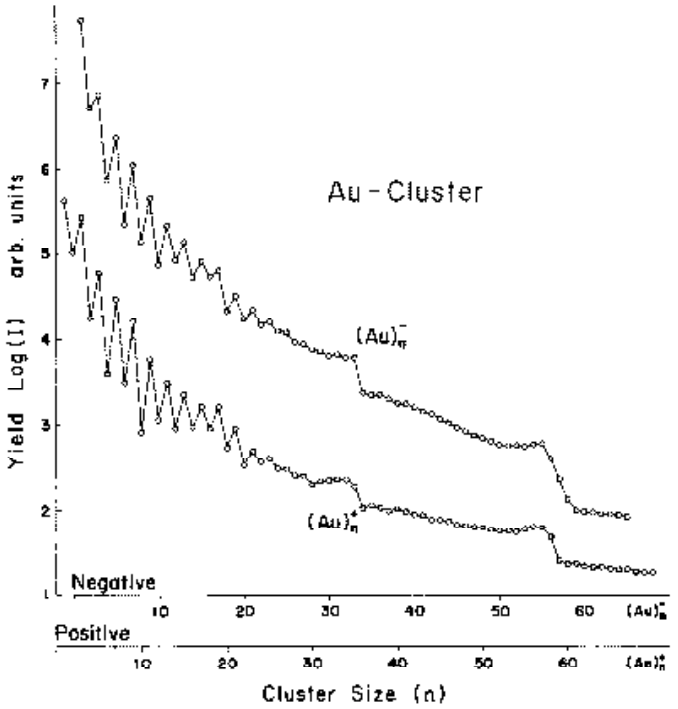

Fig. 2. Size distributions of gold clusters. $(Au)_n^-$ (upper curve) and $(Au)_n^+$ (lower curve), plotted on a logarithmic scale.

Magic clusters

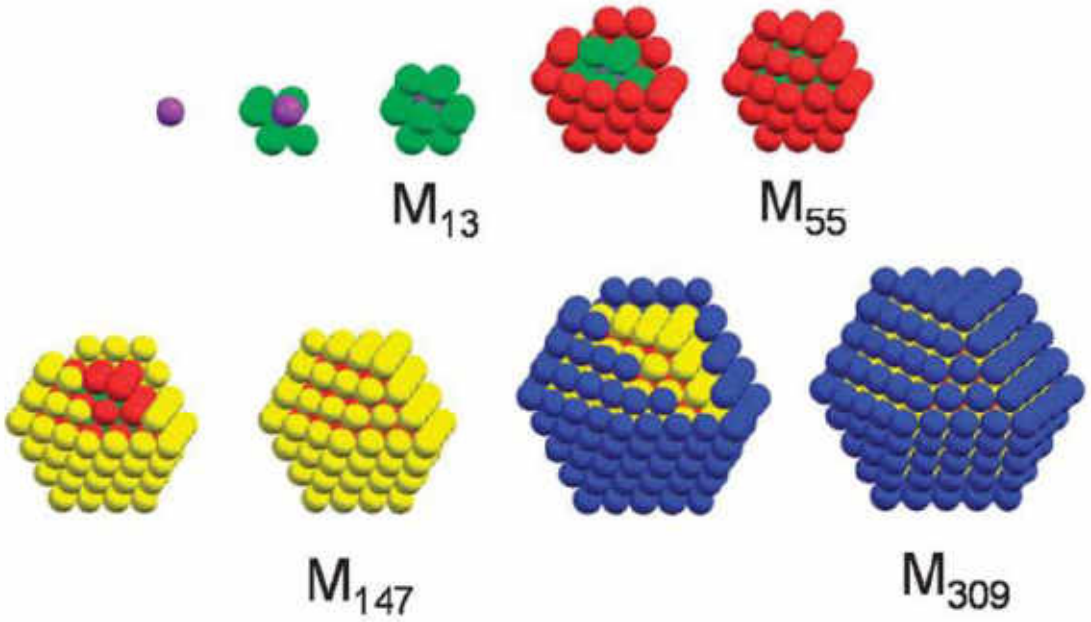

Fig. 1 Organization of full-shell clusters: a first single atom (purple) is surrounded by 12 others (green) to give a one-shell cluster M_{13}. 42 atoms (red) can be densely packed on the 12 green atoms ending with the M_{55} two-shell cluster, followed by 92 atoms (yellow) and 162 atoms (blue) to give M_{147} and M_{309}, respectively.

From Gunter Schmidt, *Chem. Soc. Rev.* **2008**, *37*, 1909–1930

C_{60}: Buckminsterfullerene

H. W. Kroto*, J. R. Heath, S. C. O'Brien, R. F. Curl & R. E. Smalley

Rice Quantum Institute and Departments of Chemistry and Electrical Engineering, Rice University, Houston, Texas 77251, USA

During experiments aimed at understanding the mechanisms by which long-chain carbon molecules are formed in interstellar space and circumstellar shells[1], graphite has been vaporized by laser irradiation, producing a remarkably stable cluster consisting of 60 carbon atoms. Concerning the question of what kind of 60-carbon atom structure might give rise to a superstable species, we suggest a truncated icosahedron, a polygon with 60 vertices and 32 faces, 12 of which are pentagonal and 20 hexagonal. This object is commonly encountered as the football shown in Fig. 1. The C_{60} molecule which results when a carbon atom is placed at each vertex of this structure has all valences satisfied by two single bonds and one double bond, has many resonance structures, and appears to be aromatic.

Fig. 1 A football (in the United States, a soccerball) on Texas grass. The C_{60} molecule featured in this letter is suggested to have the truncated icosahedral structure formed by replacing each vertex on the seams of such a ball by a carbon atom.

graphite fused six-membered ring structure. We believe that the distribution in Fig. 3*c* is fairly representative of the nascent distribution of larger ring fragments. When these hot ring clusters are left in contact with high-density helium, the clusters equilibrate by two- and three-body collisions towards the most stable species, which appears to be a unique cluster containing 60 atoms.

When one thinks in terms of the many fused-ring isomers with unsatisfied valences at the edges that would naturally arise

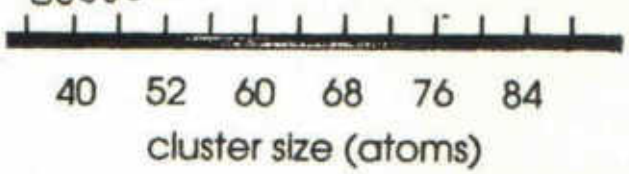

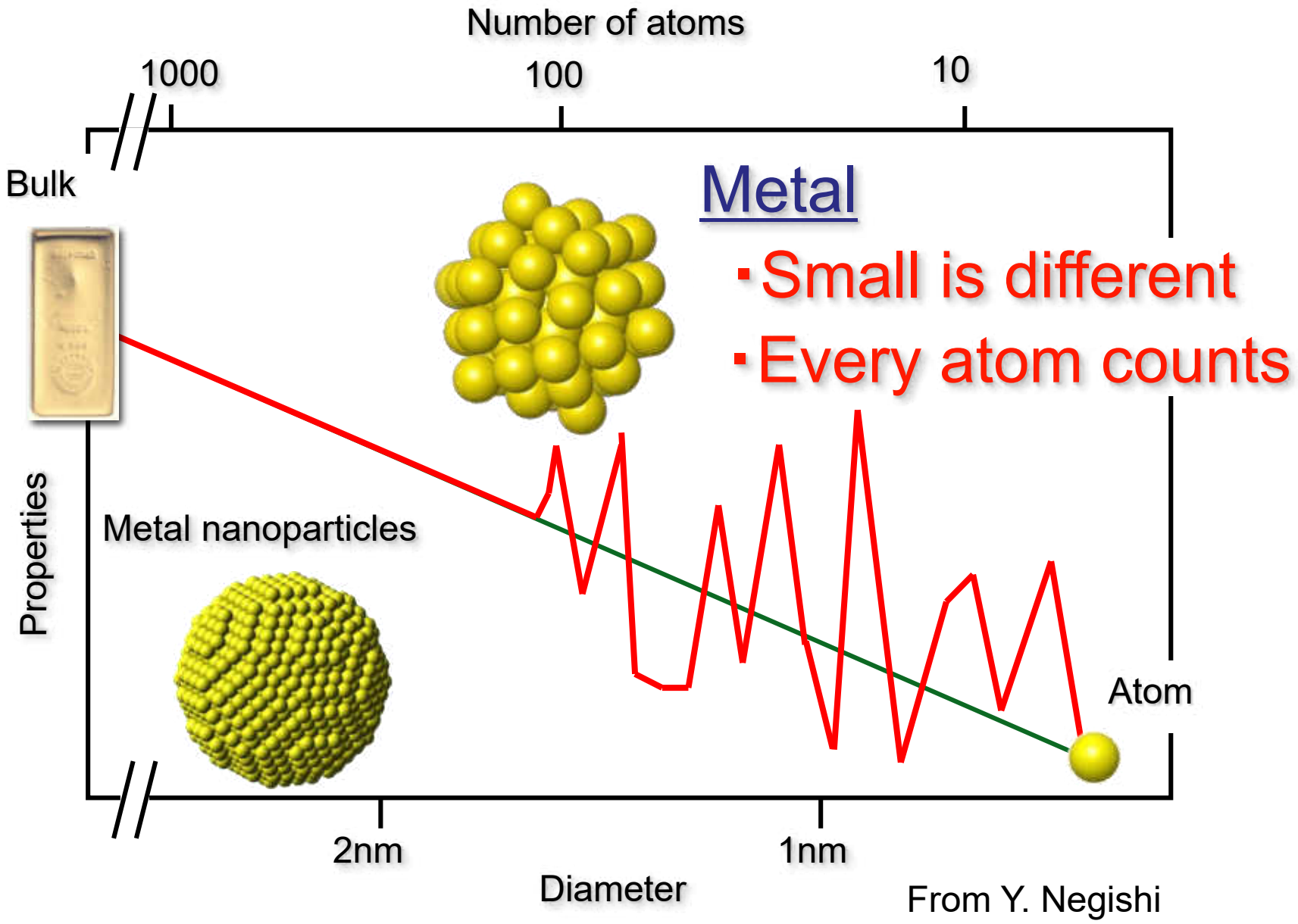
Number of atoms
1000
100
10
Bulk
Metal
Small is different
Every atom counts
Properties
Metal nanoparticles
Atom
2nm
1nm
Diameter
From Y. Negishi

Stable clusters

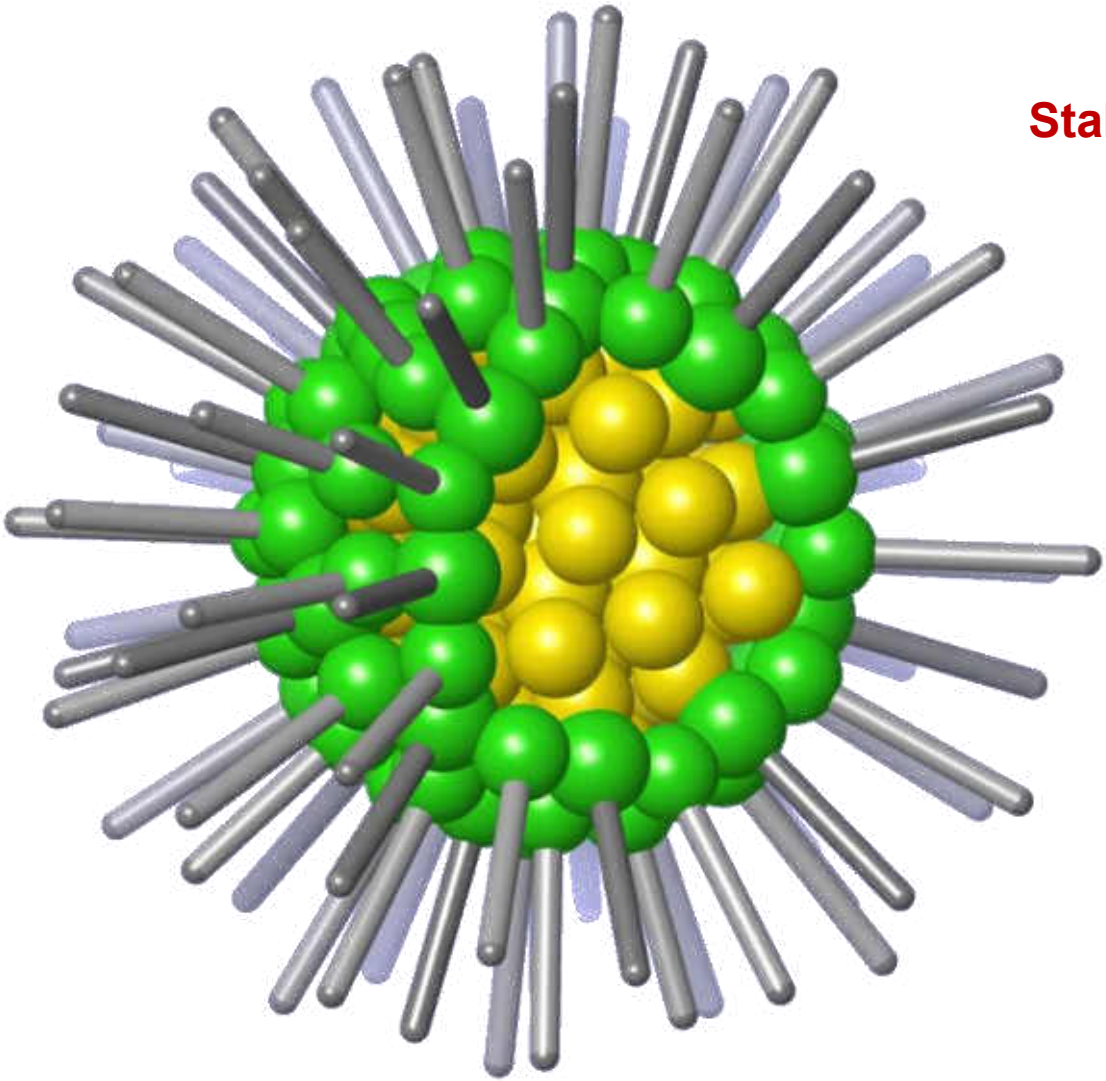

From Y. Negishi

How do we know that they exist?

Table 1 Landmark events in the history of mass spectrometry and their importance in enabling the characterization of materials

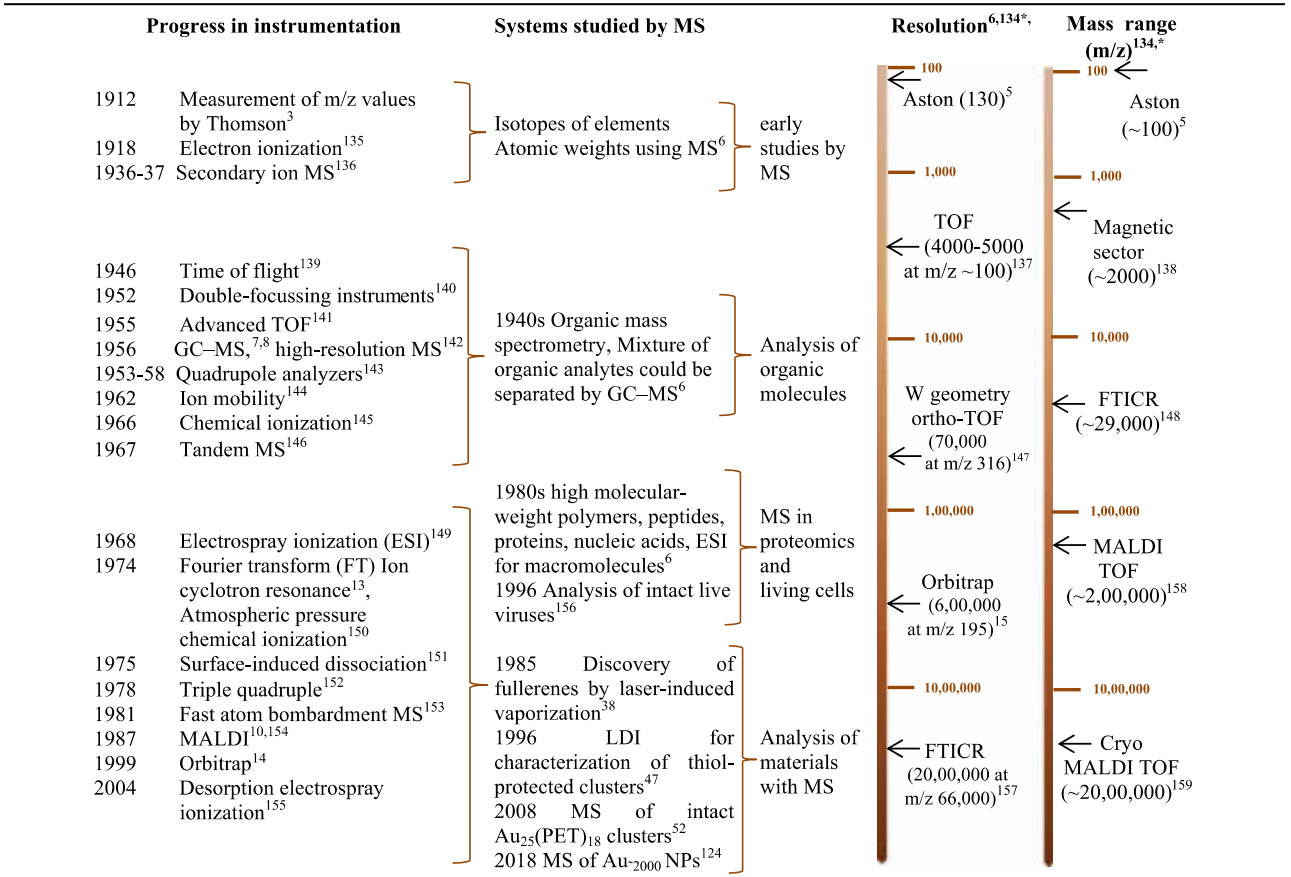

Charge detection MS

*Does not strictly correspond to the time evolution presented in the left column

Chakraborty and Pradeep *NPG Asia Materials* (2019) 11:48
https://doi.org/10.1038/s41427-019-0149-3

Synthetic methods

J. CHEM. SOC., CHEM. COMMUN., 1994 801

Synthesis of Thiol-derivatised Gold Nanoparticles in a Two-phase Liquid–Liquid System

Mathias Brust, Merryl Walker, Donald Bethell, David J. Schiffrin and Robin Whyman

Department of Chemistry, The University of Liverpool, PO Box 147, Liverpool, UK L69 3BX

Using two-phase (water–toluene) reduction of $AuCl_4^-$ by sodium borohydride in the presence of an alkanethiol, solutions of 1–3 nm gold particles bearing a surface coating of thiol have been prepared and characterised; this novel material can be handled as a simple chemical compound.

Colloidal solutions of metals have been known for a long time and a large variety of preparative techniques is now available.[1,2] Depending on the preparative conditions, the particles have a tendency to agglomerate slowly, eventually lose their dispersed character and flocculate. The removal of the solvent generally leads to the complete loss of the ability to reform a colloidal solution. Preparation of colloidal metals in a two-phase system was introduced by Faraday,[3] who reduced an aqueous gold salt with phosphorus in carbon disulfide and obtained a ruby coloured aqueous solution of dispersed gold particles. Combining this two phase approach with the more recent techniques of ion extraction and monolayer self-assembly with alkane thiols,[4] a one-step method for the preparation of an unusual new metallic material of derivatised nanometre-sized gold particles is described.

The strategy followed consisted in growing the metallic clusters with the simultaneous attachment of self-assembled thiol monolayers on the growing nuclei. In order to allow the surface reaction to take place during metal nucleation and growth, the particles were grown in a two-phase system. Two-phase redox reactions can be carried out by an appropriate choice of redox reagents present in the adjoining phases.[5] In the present case, $AuCl_4^-$ was transferred from aqueous solution to toluene using tetraoctylammonium bromide as the phase-transfer reagent and reduced with aqueous sodium borohydride in the presence of dodecanethiol ($C_{12}H_{25}SH$). On addition of the reducing agent, the organic phase changes colour from orange to deep brown within a few seconds. The overall reaction is summarized by eqns. (1) and (2), where the source of electrons is BH_4^-. The conditions of the reaction determine the ratio of thiol to gold, *i.e.* the ratio n/m. The preparation technique was as follows. An aqueous solution of hydrogen tetrachloroaurate (30 ml, 30 mmol dm^{-3}) was mixed with a solution of tetraoctylammonium bromide in toluene (80 ml, 50 mmol dm^{-3}). The two phase mixture was vigorously stirred until all the tetrachloroaurate was transferred into

$$AuCl_4^-(aq) + N(C_8H_{17})_4^+(C_7H_7Me)_{org} \rightarrow N(C_8H_{17})_4^+AuCl_4^-(C_7H_7Me) \quad (1)$$

$$mAuCl_4^-(C_7H_7Me) + nC_{12}H_{25}SH(C_7H_8Me) + 3ne^- \rightarrow 4mCl^-(aq) + (Au_m)(C_{12}H_{25}SH)_n(C_7H_7Me) \quad (2)$$

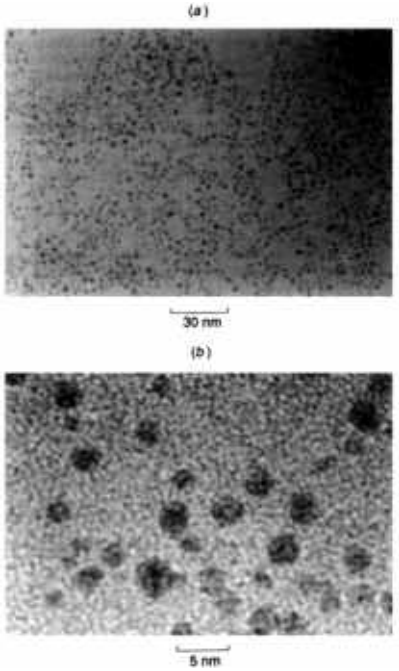

Fig. 1 TEM pictures of the thiol derivatised gold nanoparticles: (a) low and (b) high magnification

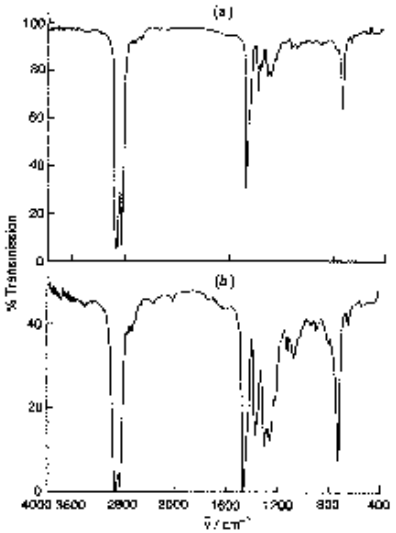

Fig. 2 IR spectra of (a) dodecanethiol and (b) nanoparticles prepared in the present work. The particles were deposited from $CHCl_3$ solution by evaporation of a drop of a toluene solution.

Observing such clusters

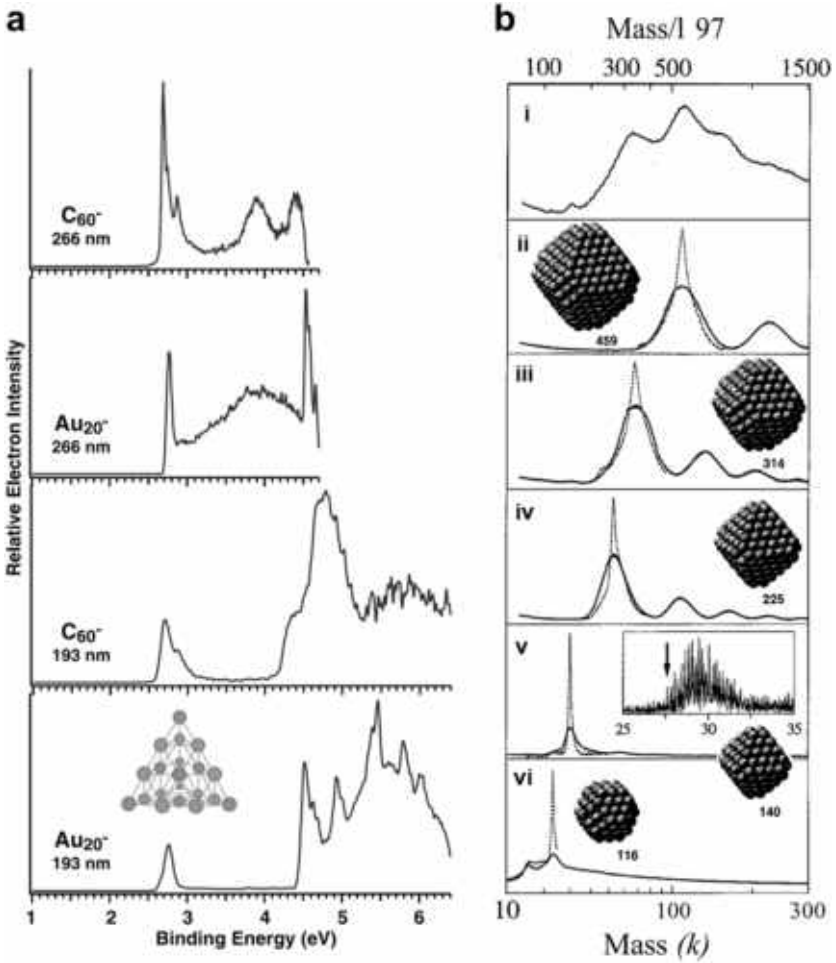

Fig. 2 Early stages of MS of noble metal clusters. a Photoelectron spectra of Au_{20}^- cluster compared with C_{60}^- at 193 nm and 266 nm[45]. (Copyright© 2003 the American Association for the Advancement of Science) **b** Mass spectra obtained by laser desorption ionization of dodecanethiol thiol-protected gold clusters, (i) crude mixture of clusters and (ii–vi) separated fractions[47]. (Copyright© 1996 John Wiley and Sons)

Chakraborty and Pradeep *NPG Asia Materials* (2019) 11:48
https://doi.org/10.1038/s41427-019-0149-3

Atomically precise metal clusters as materials

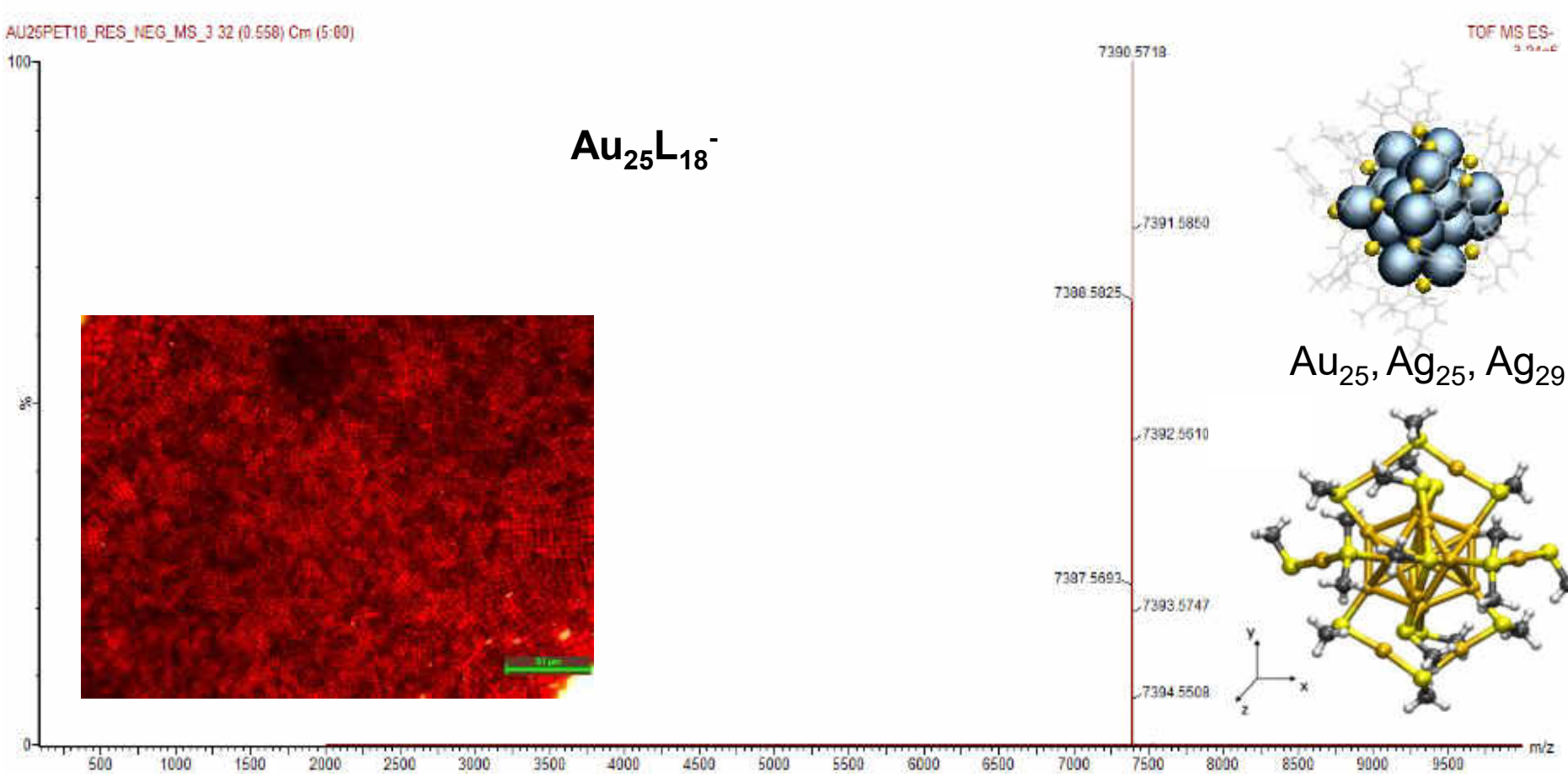

T. Pradeep et. al. *Acc. Chem. Res.* 2018; 2019.

Structures

$Au_{25}(SR)_{18}$

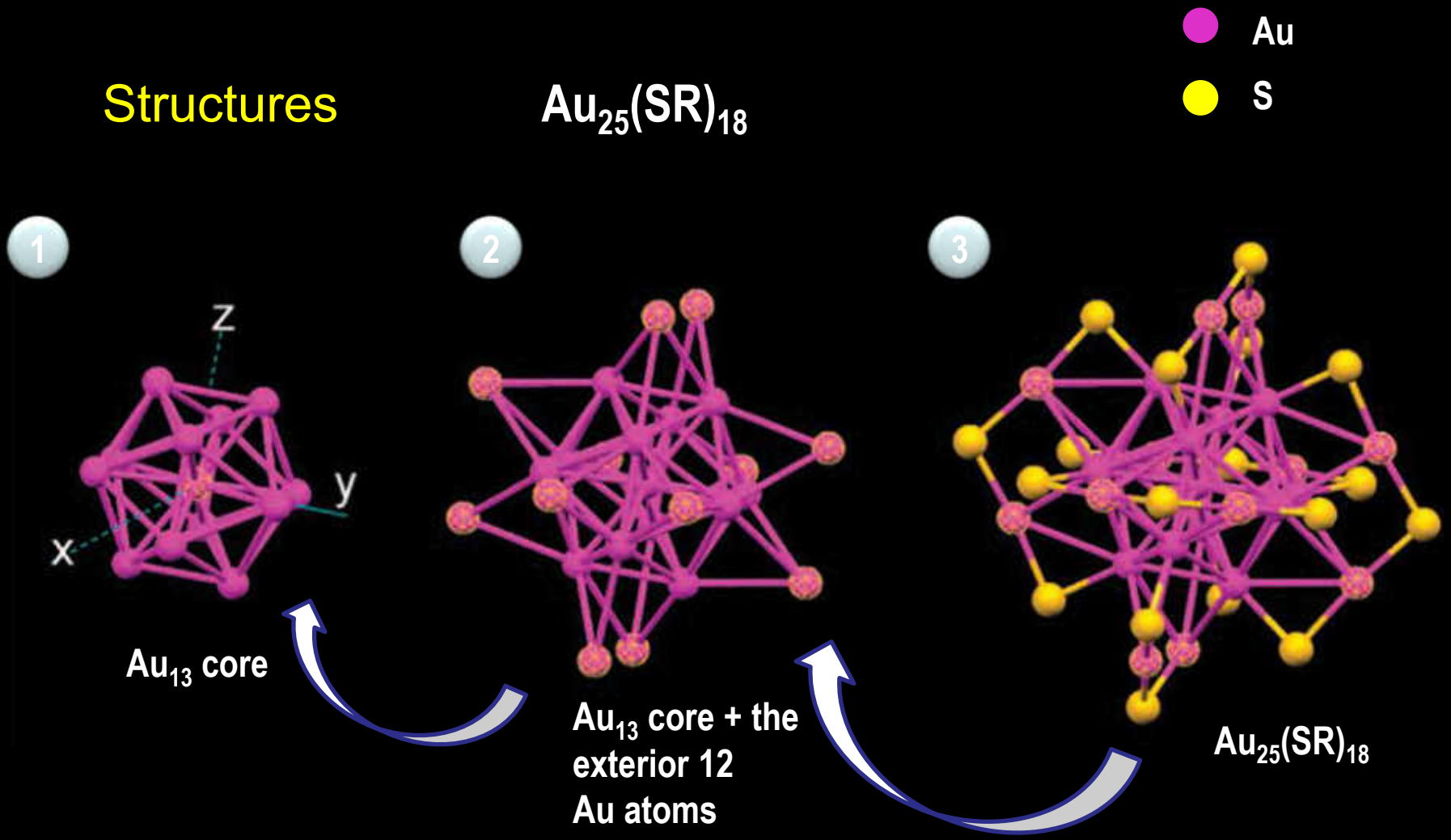

>150 such clusters

Zhu, M.; Aikens, C. M.; Hollander, F. J.; Schatz, G. C.; Jin, R. *J. Am. Chem. Soc.* **2008**, *130*, 5883-5885.

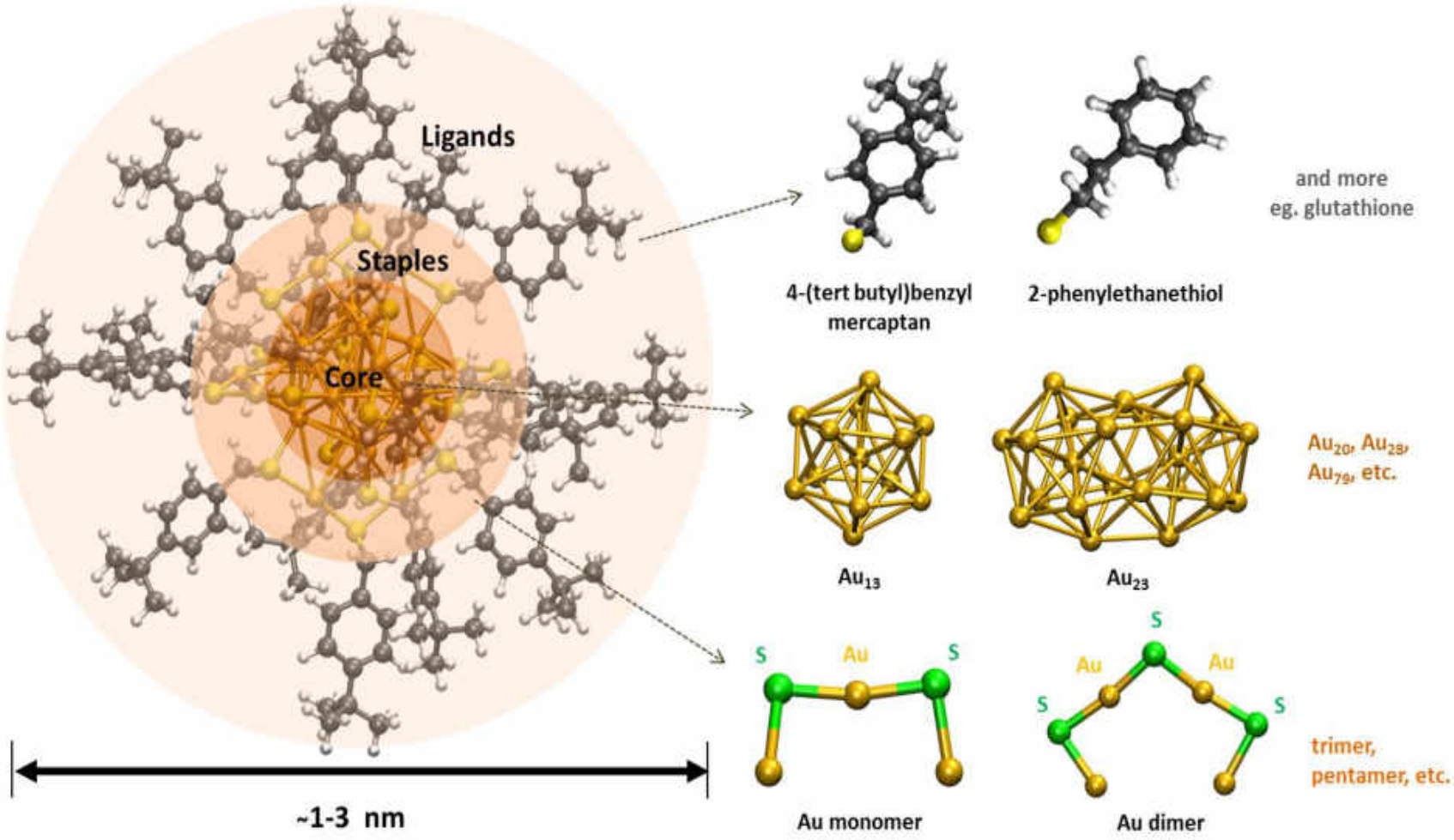
Ligands
Staples
Core
~1-3 nm
4-(tert butyl)benzyl mercaptan
2-phenylethanethiol
and more
eg. glutathione
Au13
Au23
Au20, Au28,
Au79, etc.
S
Au
S
Au monomer
S
Au
Au
S
S
Au dimer
trimer,
pentamer, etc.

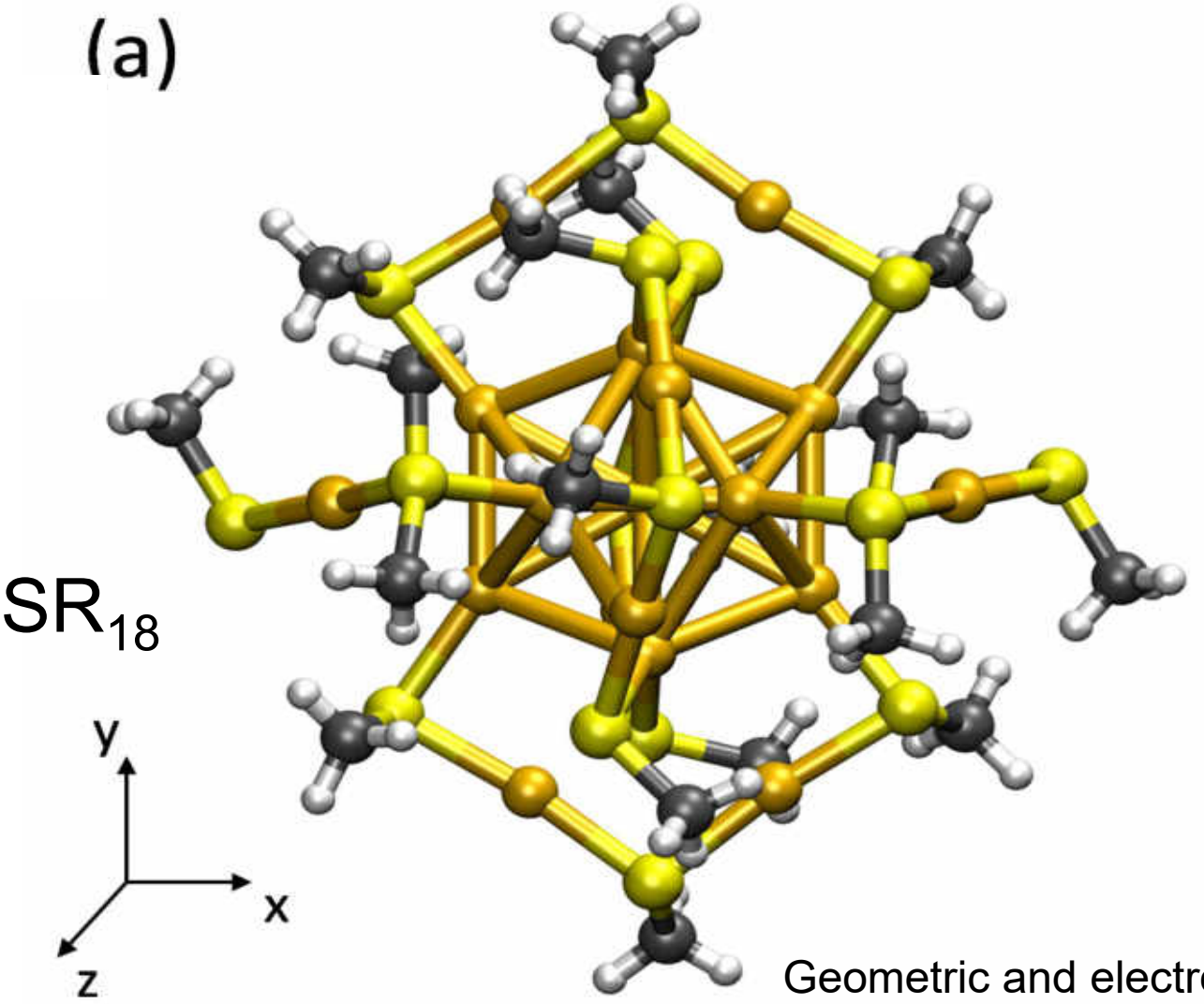

$Au_{25}SR_{18}$

Geometric and electronic stability

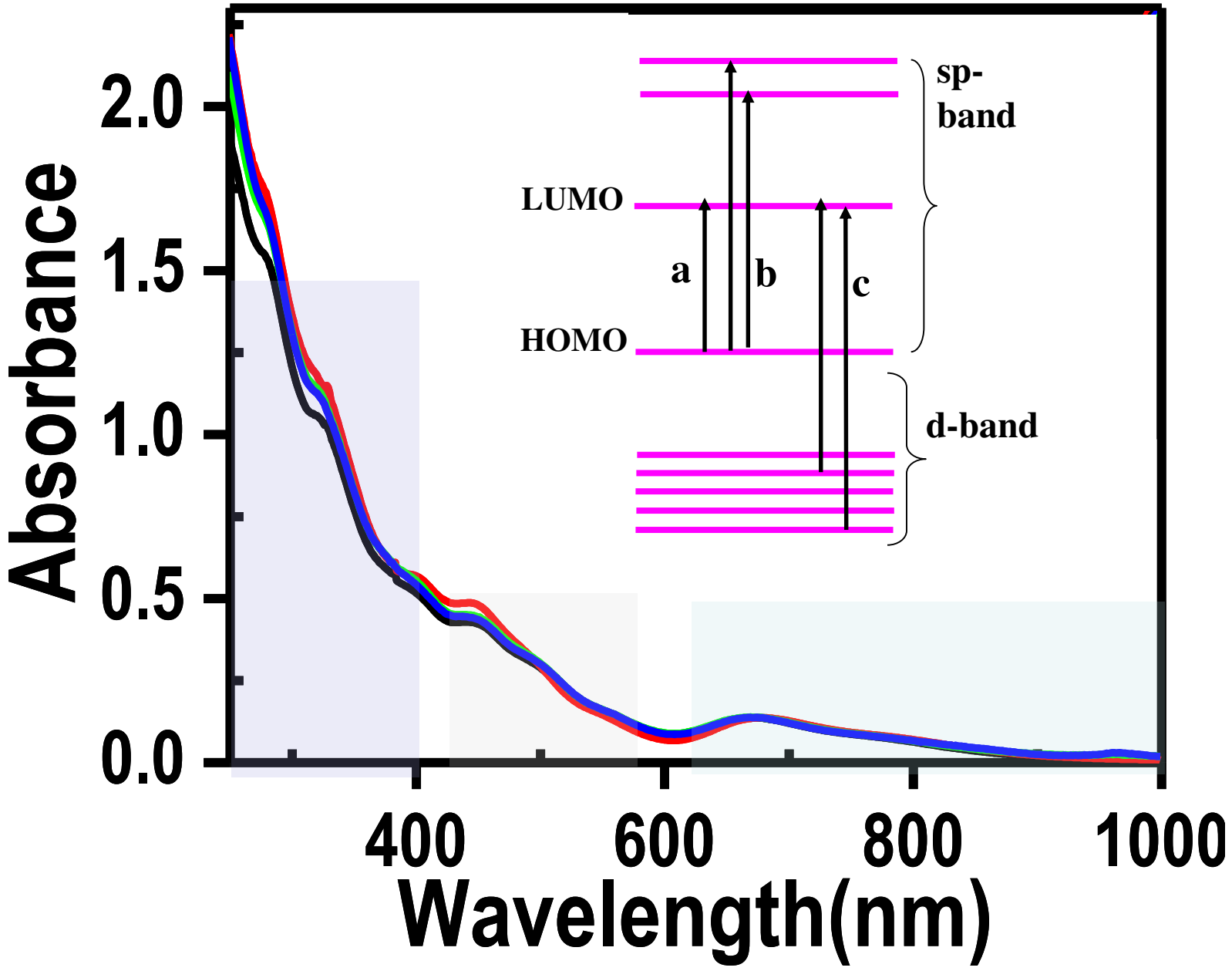
Absorbance
2.0
1.5
1.0
0.5
0.0
400
600
800
1000
Wavelength(nm)
sp-
band
LUMO
a
b
c
HOMO
d-band

Ligand Exchange of $Au_{25}SG_{18}$ Leading to Functionalized Gold Clusters: Spectroscopy, Kinetics, and Luminescence

E. S. Shibu,[†] M. A. Habeeb Muhammed,[†] T. Tsukuda,[‡] and T. Pradeep*[,†]

DST Unit on Nanoscience (DST UNS), Department of Chemistry and Sophisticated Analytical Instrument Facility, Indian Institute of Technology, Madras, Chennai 600 036, India and Institute for Molecular Science, Myodaiji, Okazaki 444-8585, Japan

Received: January 18, 2008;

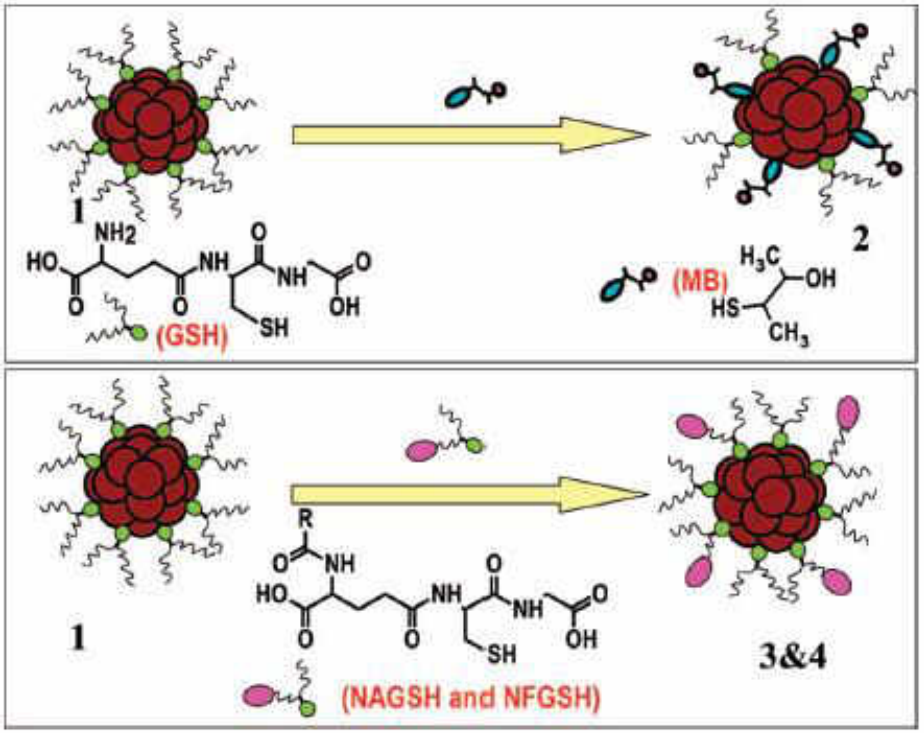

With Tatsuya Tsukuda

Evolution of noble metal clusters

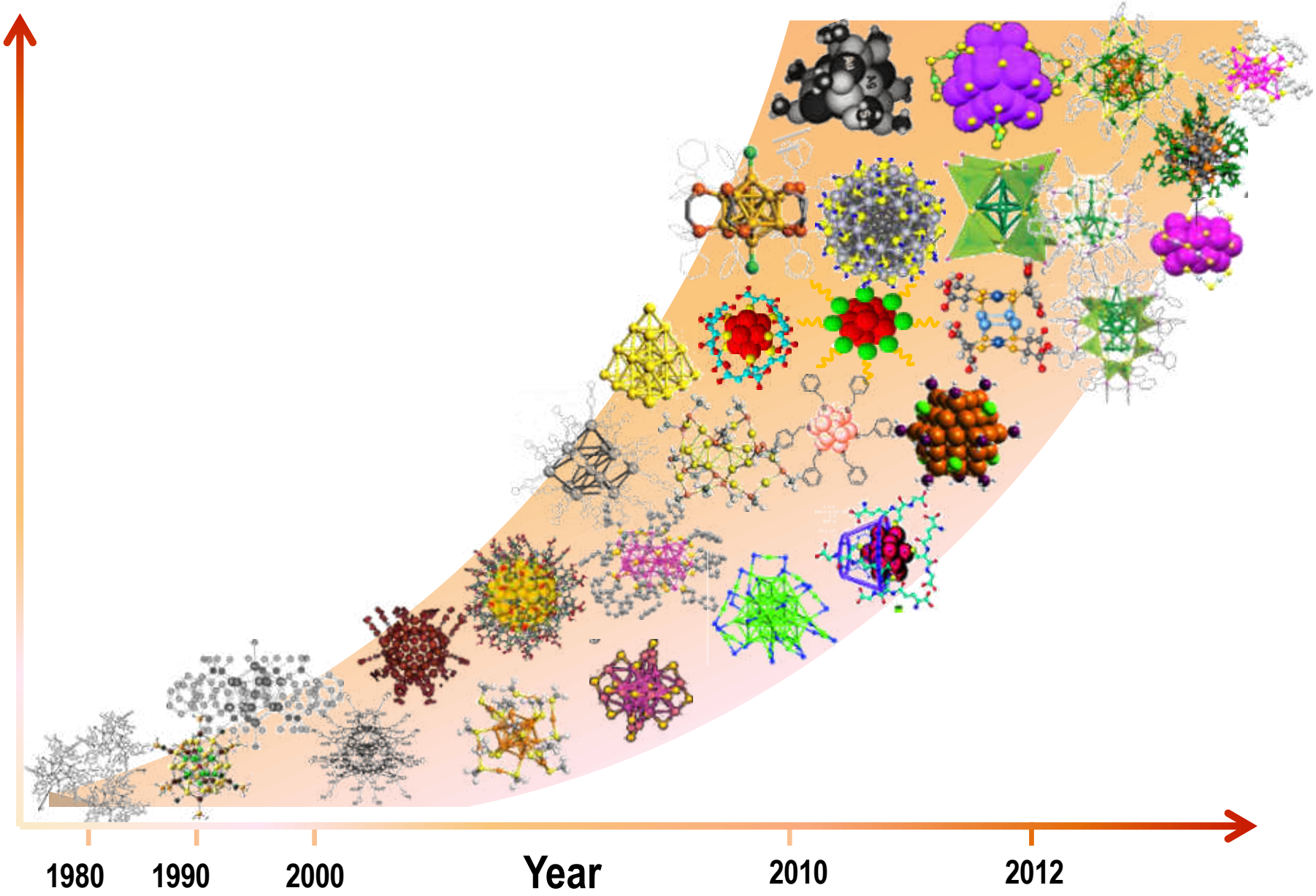

I. Chakraborty and T. Pradeep, *Chem. Rev.* 2017

Mass spectrometry and materials science

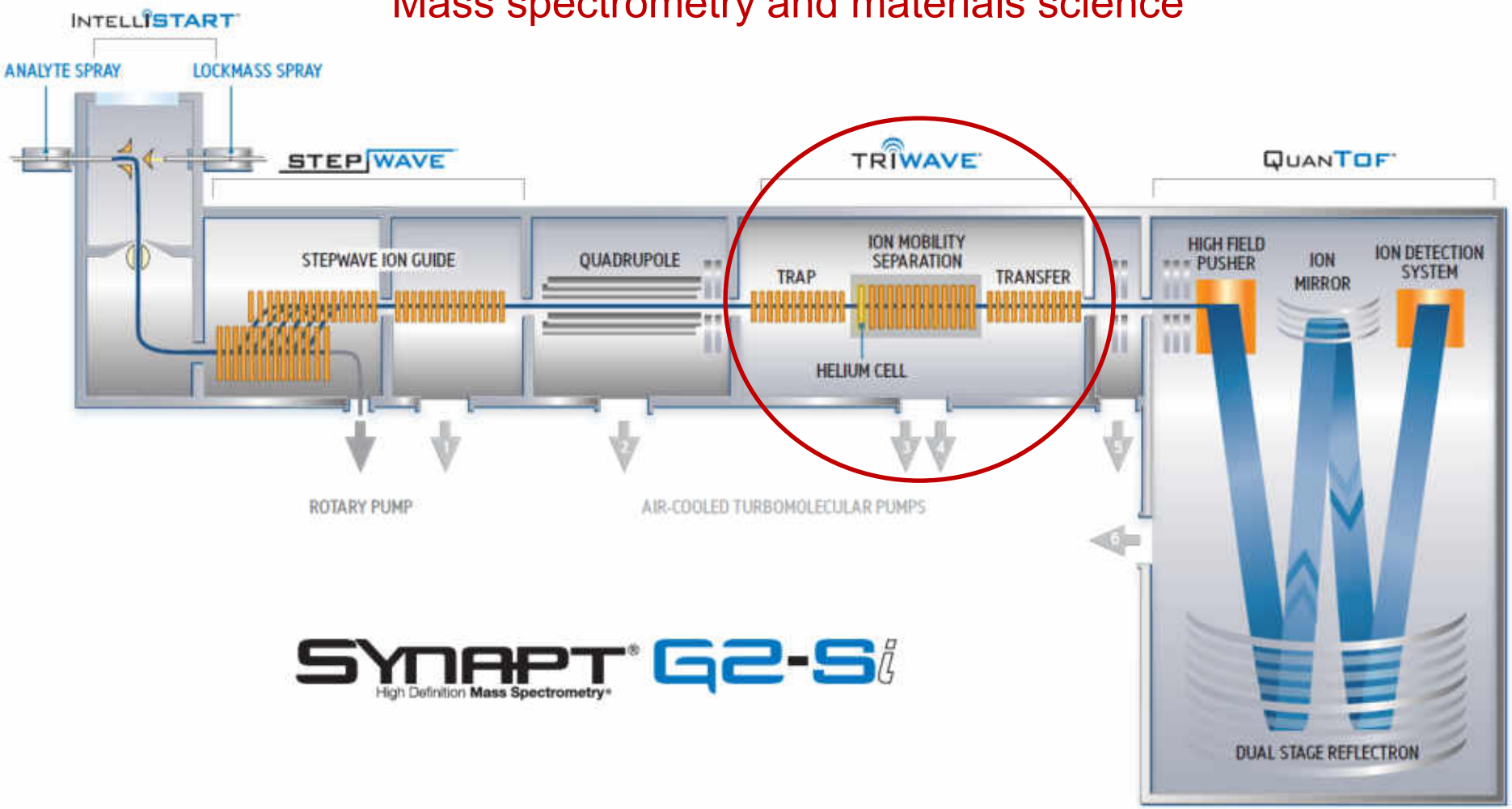

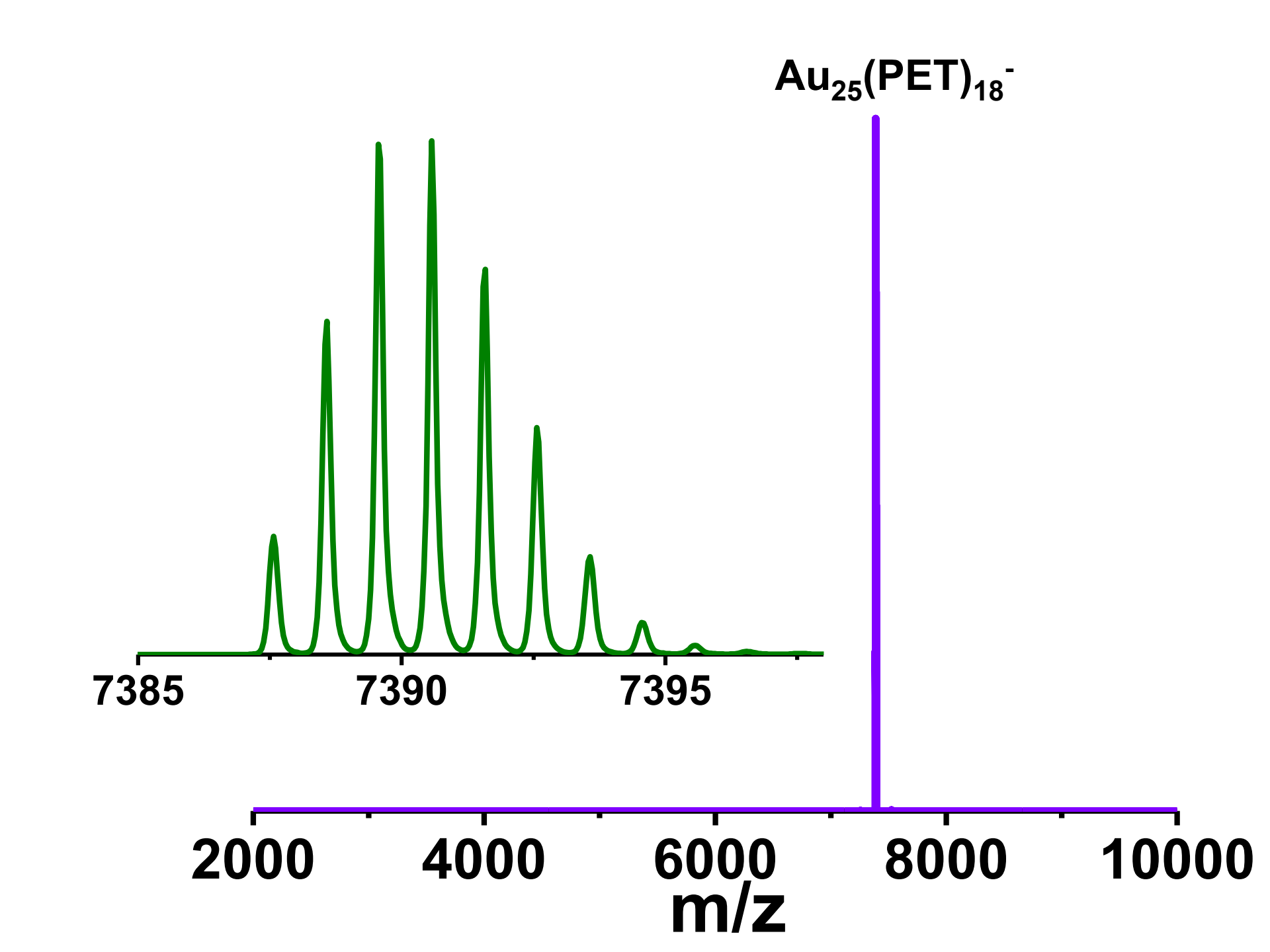
Au25(PET)18-
7385
7390
7395
2000
4000
6000
8000
10000
m/z

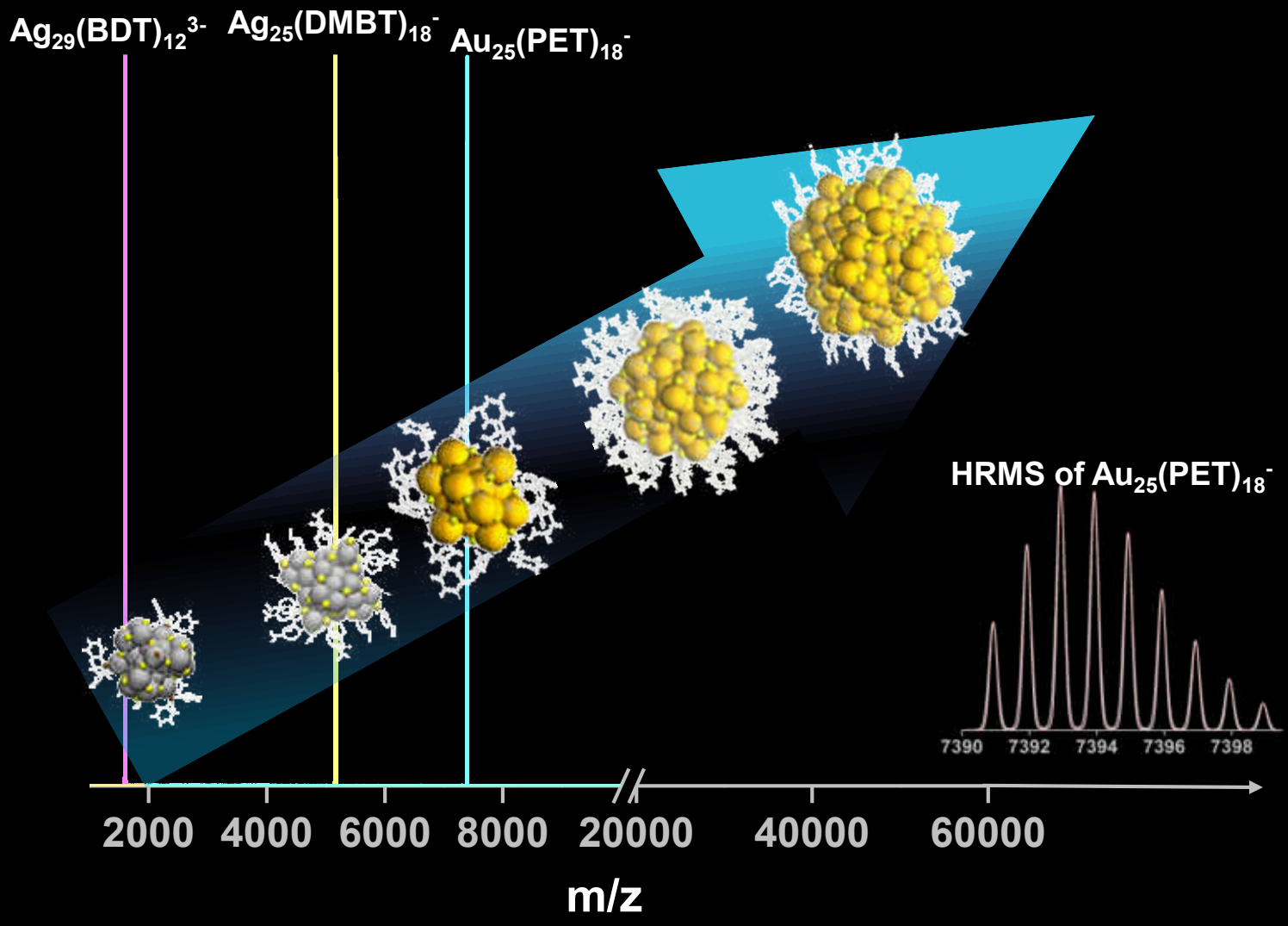
$Ag_{29}(BDT)_{12}^{3-}$
$Ag_{25}(DMBT)_{18}^{-}$
$Au_{25}(PET)_{18}^{-}$
HRMS of $Au_{25}(PET)_{18}^{-}$
7390
7392
7394
7396
7398
2000
4000
6000
8000
20000
40000
60000
m/z

Molecular materials

ACCOUNTS
of chemical research

Article

pubs.acs.org/accounts

Approaching Materials with Atomic P… lar Cluster Assemblies

Papri Chakraborty, Abhijit Nag, Amrita Chakraborty, and…

DST Unit of Nanoscience (DST UNS) and Thematic Unit of Excellen… of Technology Madras, Chennai 600 036, India

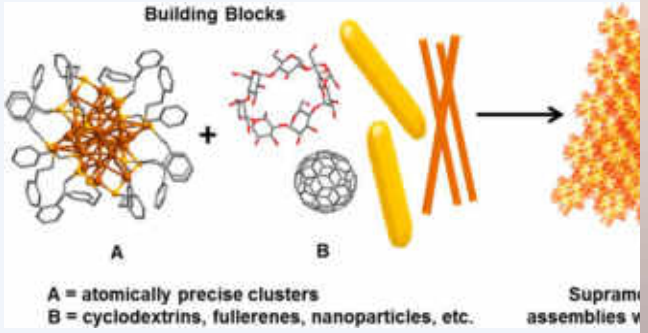

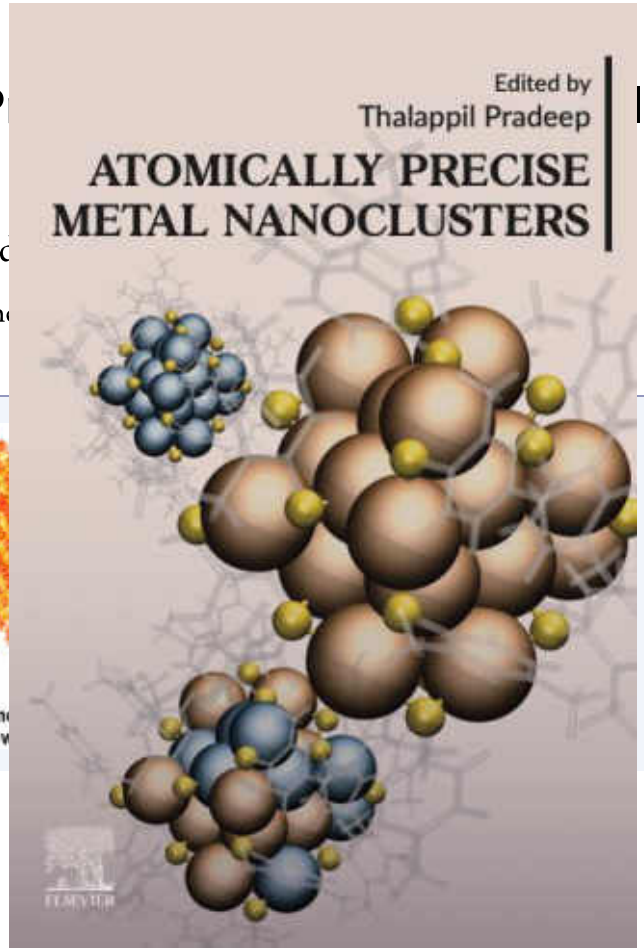

Molecules and their properties

Chemical formula	H_2O
Molecular weight	18.0148
Critical temperature	373.91°C
Critical pressure	22.05 MPa
Critical density	315.0 kg/m^3
Triple point temperature	0.01°C
Triple point pressure	615.066 Pa
Normal boiling point	100.0°C
Normal freezing point	0.0°C
Density of ice at normal melting point	918.0 kg/m^3
Maximum density, 3.98°C	999.973 kg/m^3
Viscosity, 25°C	0.889 mN s/m^2
Surface tension, 25°C	72 mN/m
Heat Capacity, 25°C	4.1796 kJ/kg.K
Enthalpy of vaporisation, 100°C	2,257.7 kJ/kg
Enthalpy of fusion, 0°C	333.8 kJ/kg
Velocity of sound, 0°C	1.403 km/s
Dielectric constant, 25°C	78.40
Electrical conductivity, 25°C	8 µS/m
Refractive index, 25°C	1.333
Liquid compressibility, 10°C	480. × 10^{-12}m^2/N
Coefficient of thermal expansion, 25°C	256.32 × 10^{-6} K^{-1}
Thermal Conductivity, 25°C	0.608 W/m.K

Molecular formula
Molecular weight
Molecular structure
Molecular absorption and emission
Molecular reactions
Molecular assembly
Molecular co-crystals
Ionization potential
Electron affinity

Phases - phase transitions
Physical properties
Electrical, magnetic
Mechanical properties
Electrochemical properties

Future?

Molecular reactions

Reactions on clusters

Reactions between clusters

Inter-cluster reactions

JACS
JOURNAL OF THE AMERICAN CHEMICAL SOCIETY

Article

pubs.acs.org/JACS

Intercluster Reactions between $Au_{25}(SR)_{18}$ and $Ag_{44}(SR)_{30}$

K. R. Krishnadas, Atanu Ghosh, Ananya Baksi, Indranath Chakraborty,† Ganapati Natarajan, and Thalappil Pradeep*

DST Unit of Nanoscience (DST UNS) and Thematic Unit of Excellence, Department of Chemistry, Indian Institute of Technology Madras, Chennai, 600 036, India

Supporting Information

$A + B \rightarrow C + D$

$Au_{25}(FTP)_{18} + Ag_{44}(FTP)_{30} \longrightarrow Au_{25-x}Ag_x(FTP)_{18}$

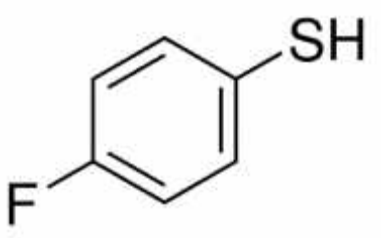

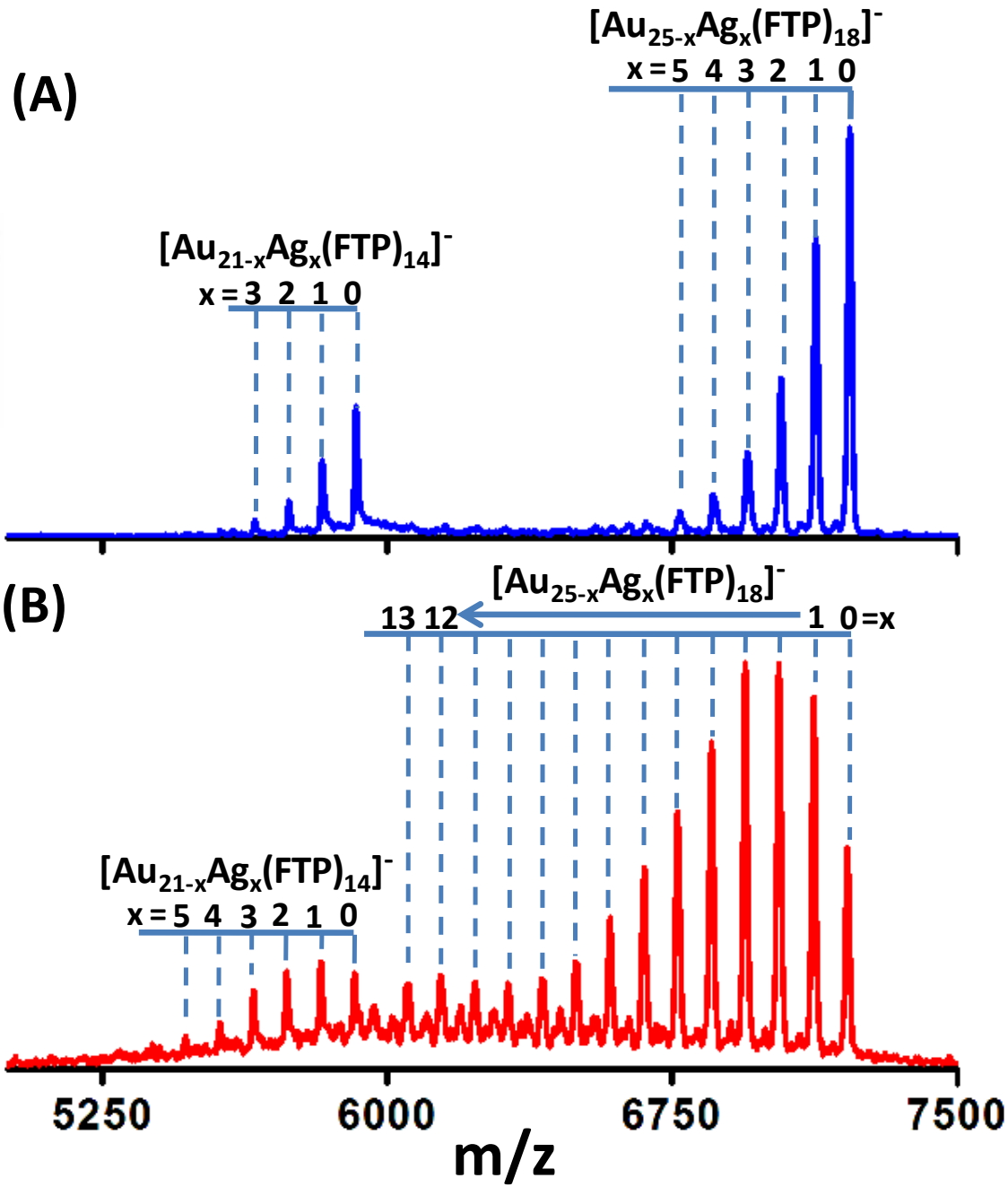

Ag_{25}-Au_{25} experiments

K. R. Krishnadas et al. *Nature Commun.* 2016

Reaction between $Au_{25}(PET)_{18}$ and $Ag_{25}(DMBT)_{18}$

DMBT

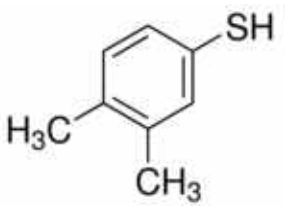

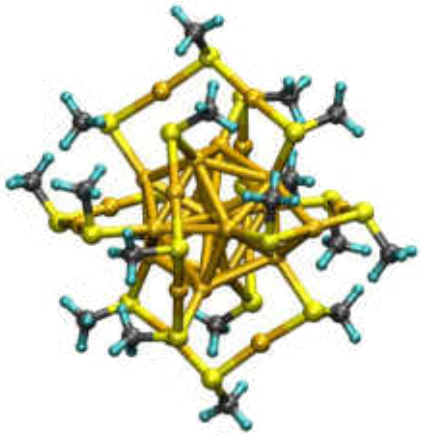

PET

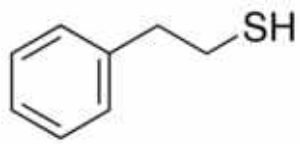

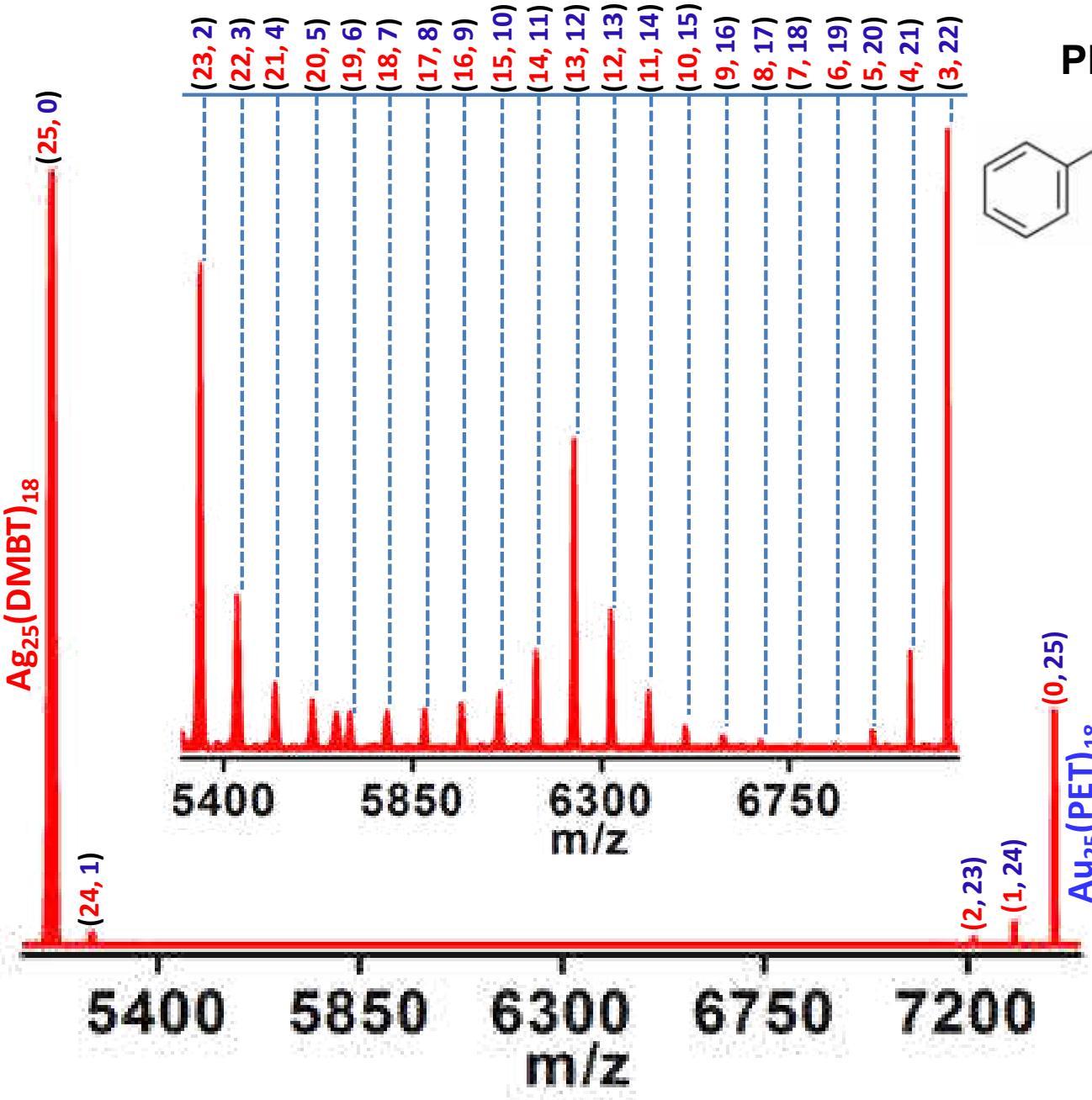

$[Ag_{25}(DMBT)_{18}+Au_{25}(PET)_{18}]^{2-}$

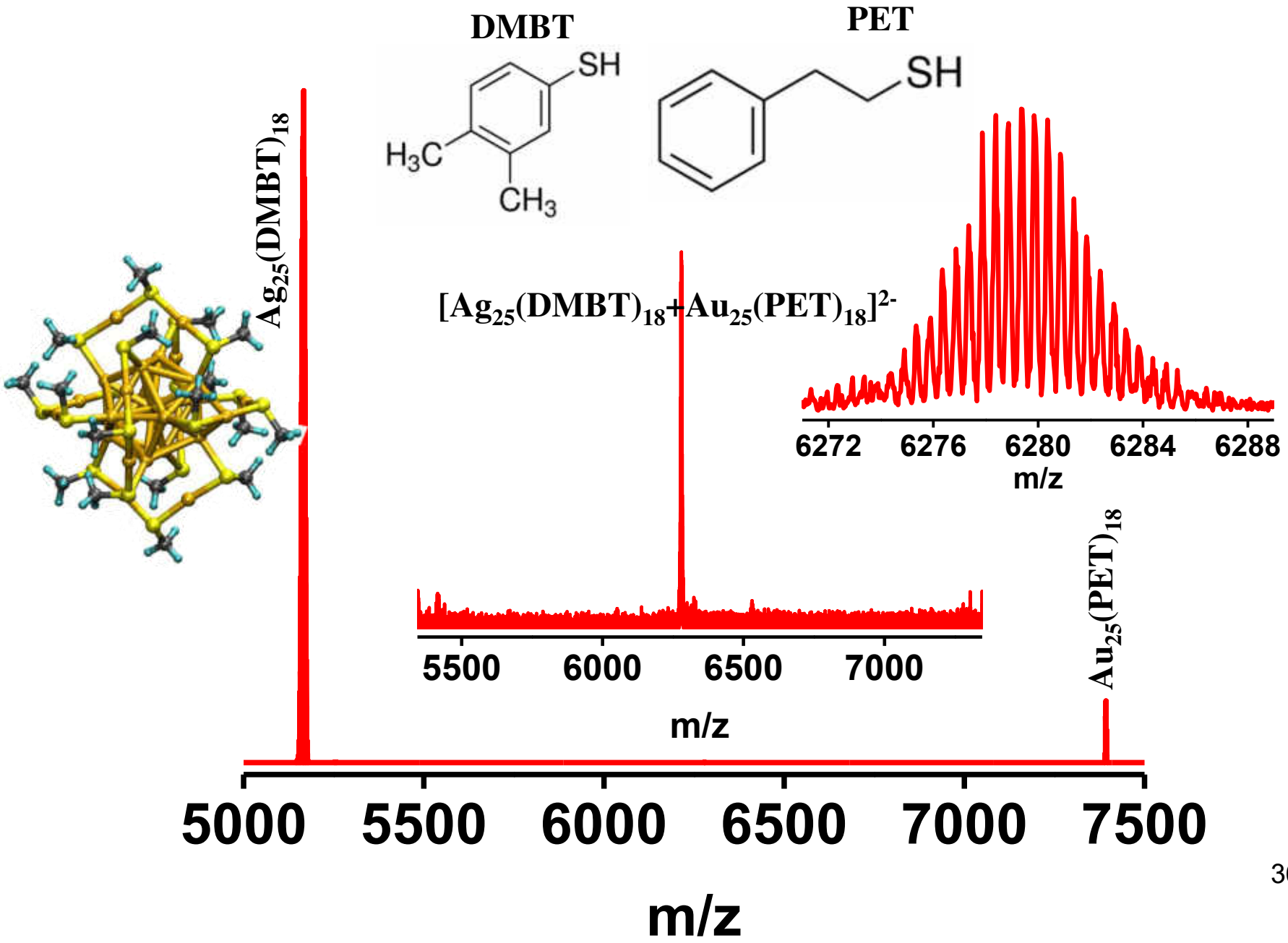

Evolution of alloy clusters from the dianionic adduct, $[Ag_{25}Au_{25}(DMBT)_{18}(PET)_{18}]^{2-}$

$Ag_{25}(DMBT)_{18}$:$Au_{25}(PET)_{18}$
0.3:1.0

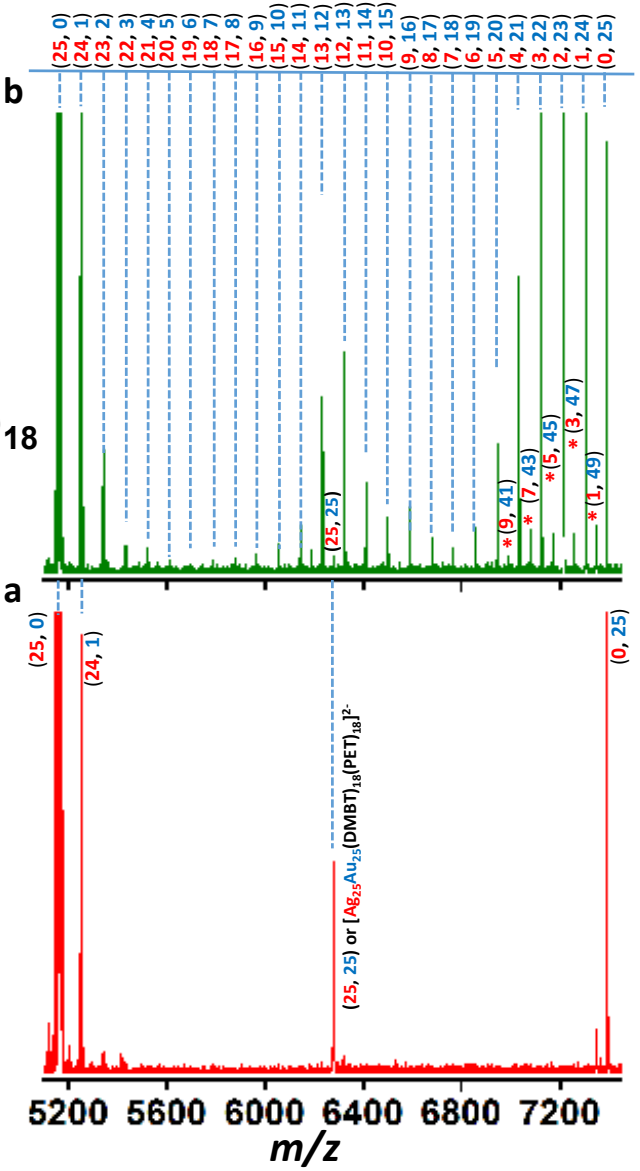

within 5 min

within 2 min

Optimized structure of $[Ag_{25}Au_{25}(DMBT)_{18}(PET)_{18}]^{2-}$

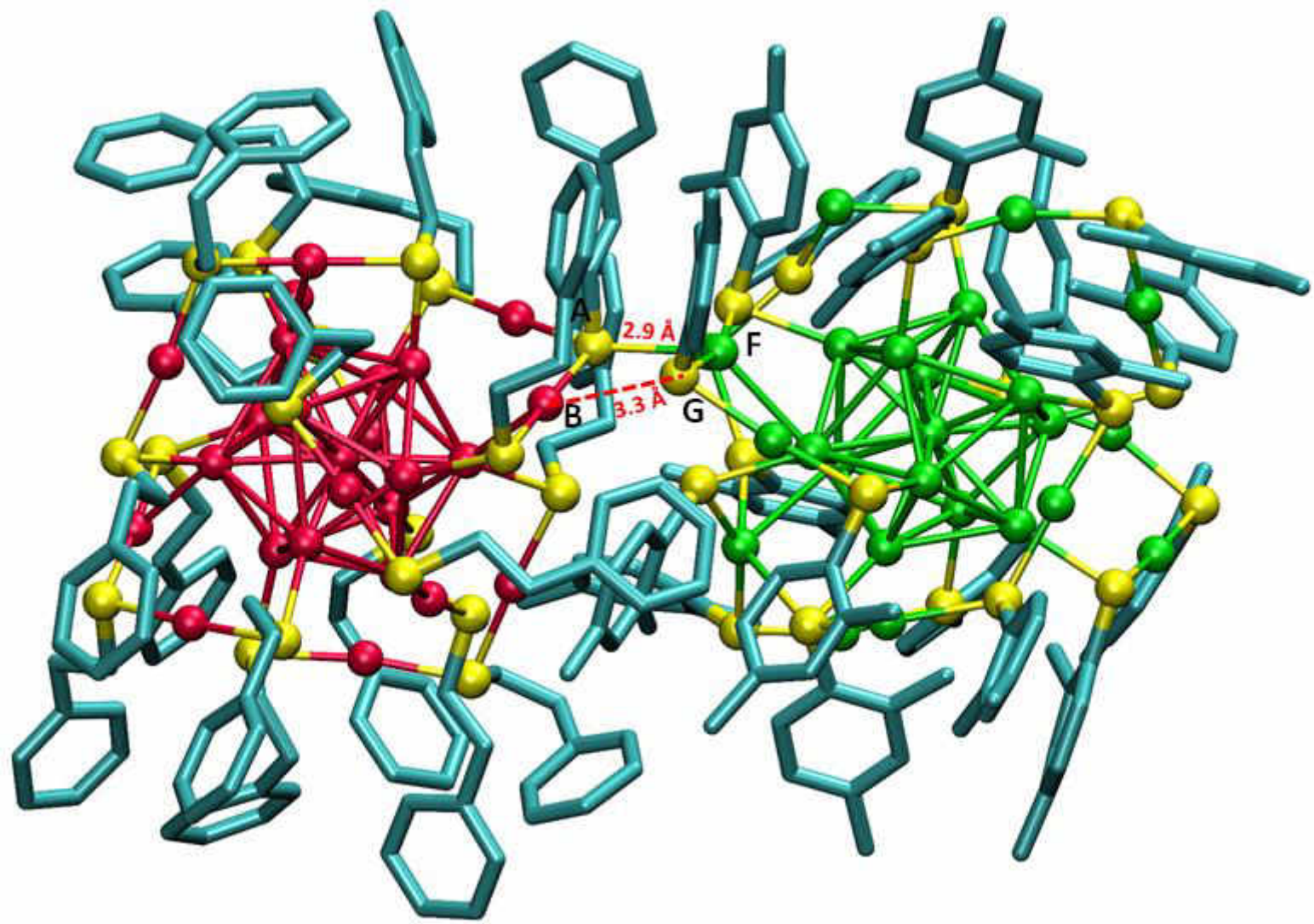

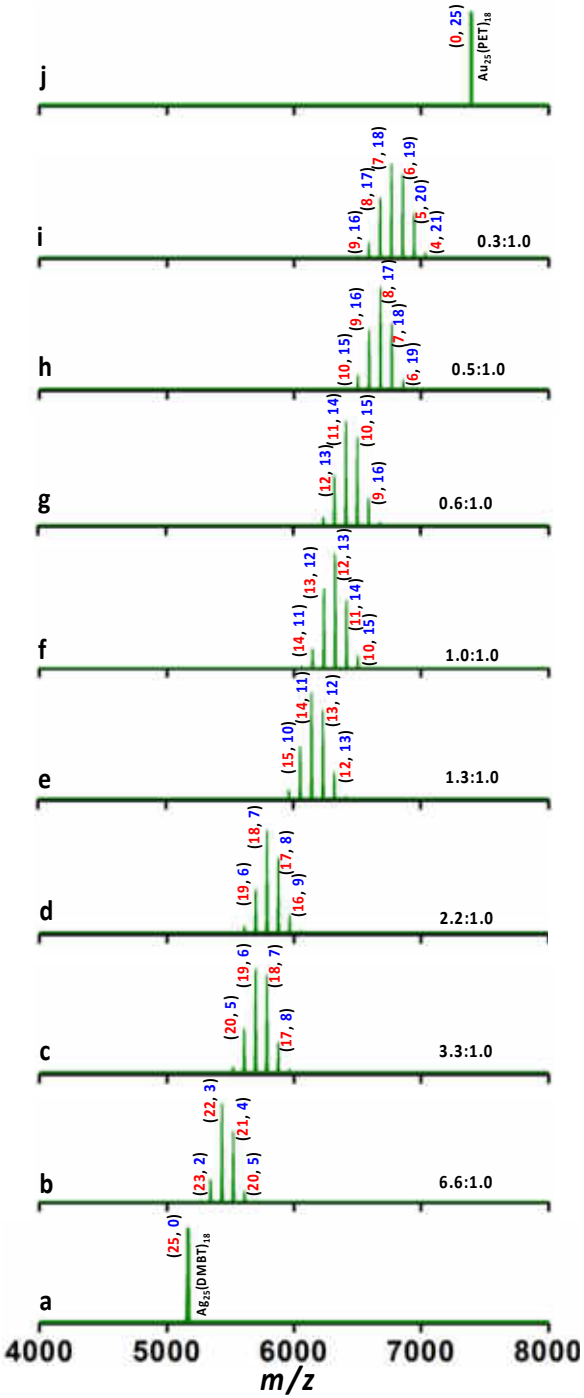
j
(0, 25)
Au25(PET)18
i
(9, 16)
(8, 17)
(7, 18)
(6, 19)
(5, 20)
(4, 21)
0.3:1.0
h
(10, 15)
(9, 16)
(8, 17)
(7, 18)
(6, 19)
0.5:1.0
g
(12, 13)
(11, 14)
(10, 15)
(9, 16)
0.6:1.0
f
(14, 11)
(13, 12)
(12, 13)
(11, 14)
(10, 15)
1.0:1.0
e
(15, 10)
(14, 11)
(13, 12)
(12, 13)
1.3:1.0
d
(19, 6)
(18, 7)
(17, 8)
(16, 9)
2.2:1.0
c
(20, 5)
(19, 6)
(18, 7)
(17, 8)
3.3:1.0
b
(23, 2)
(22, 3)
(21, 4)
(20, 5)
6.6:1.0
a
(25, 0)
Ag25(DMBT)18
4000
5000
6000
7000
8000
m/z

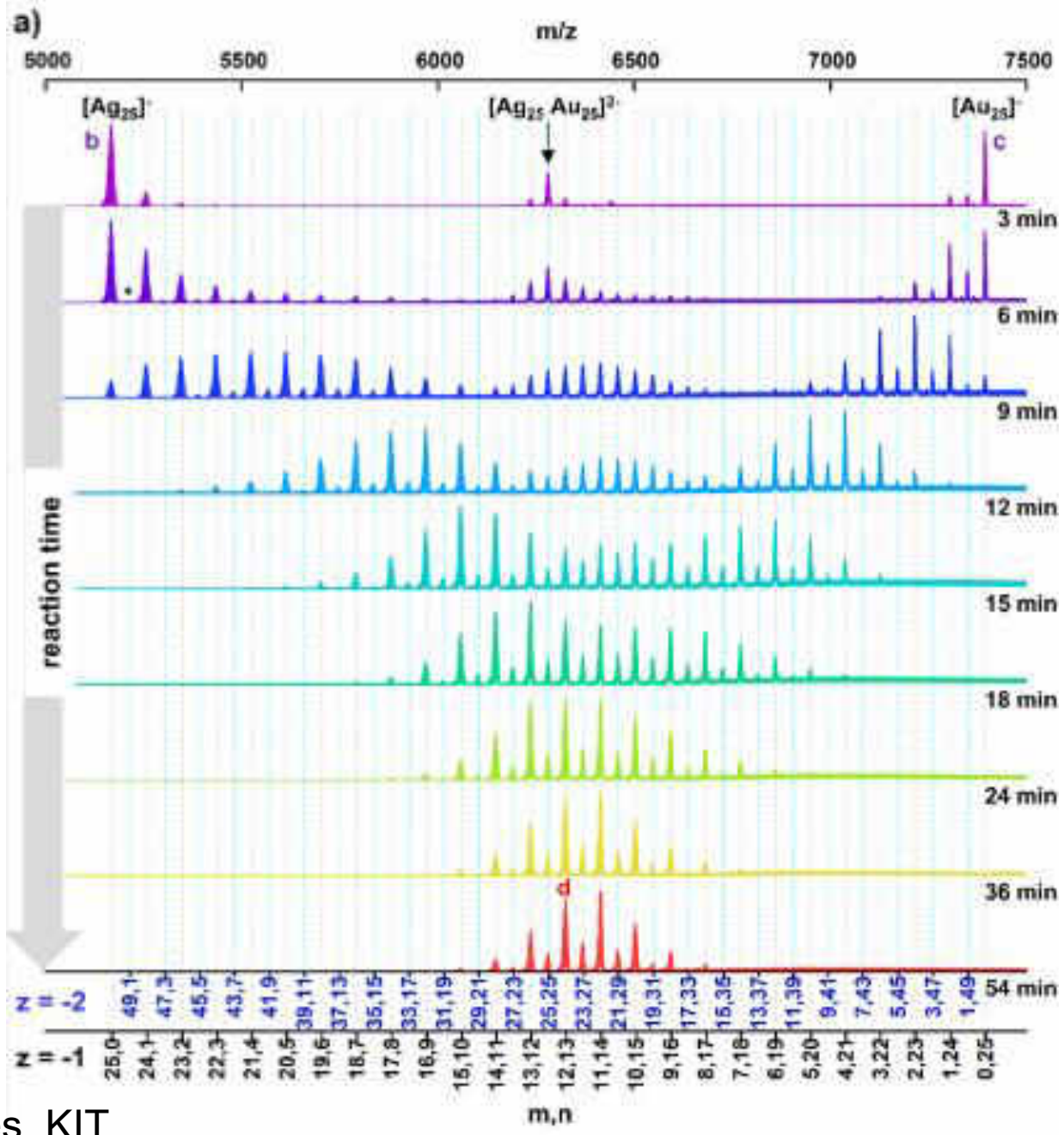

Manfred Kappes, KIT

M. Neumaier, A. Baksi, et. al., *JACS* 2021

Kinetics of the exchange (monitored on the Ag_{25} side)

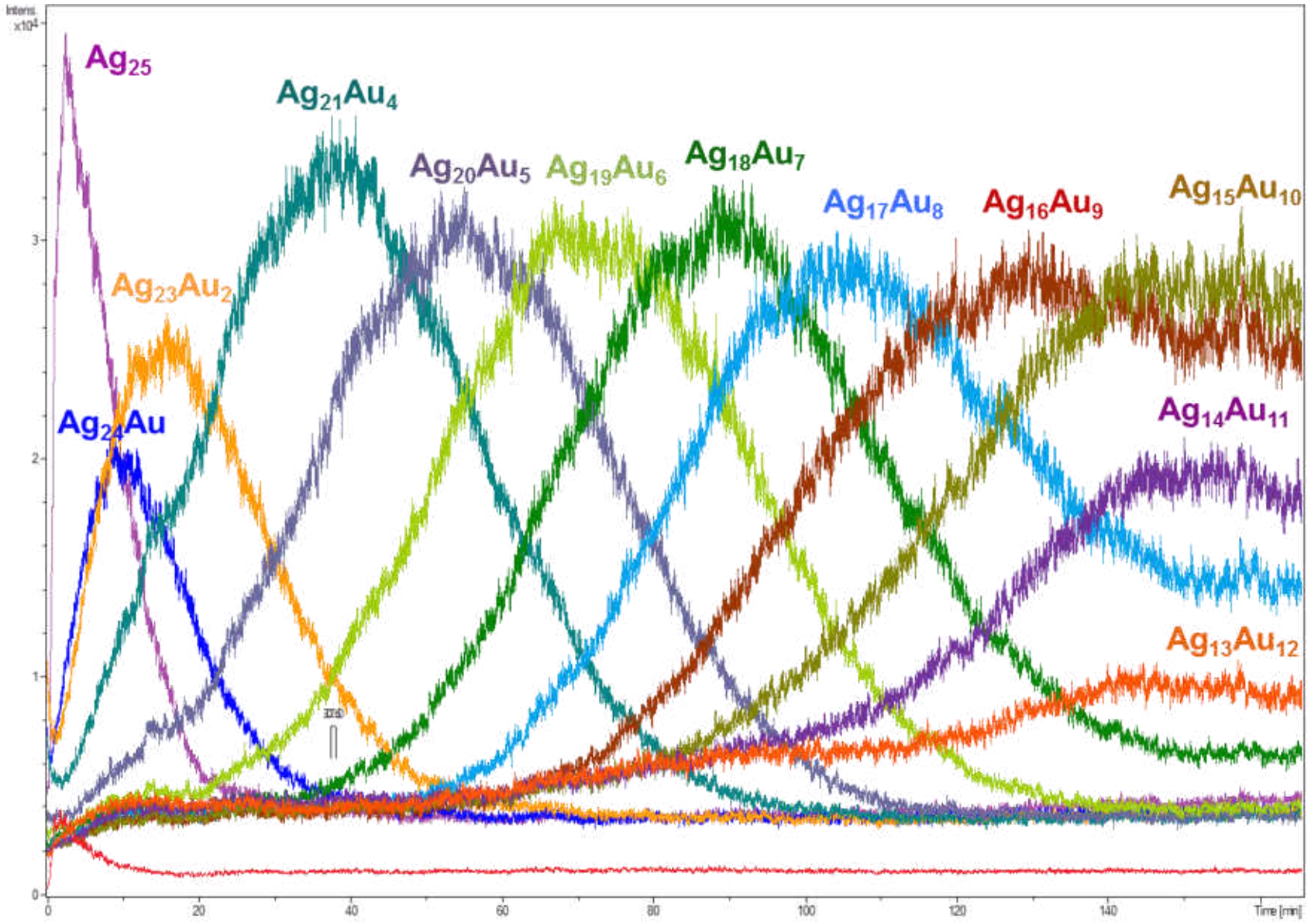

Isotopic exchange

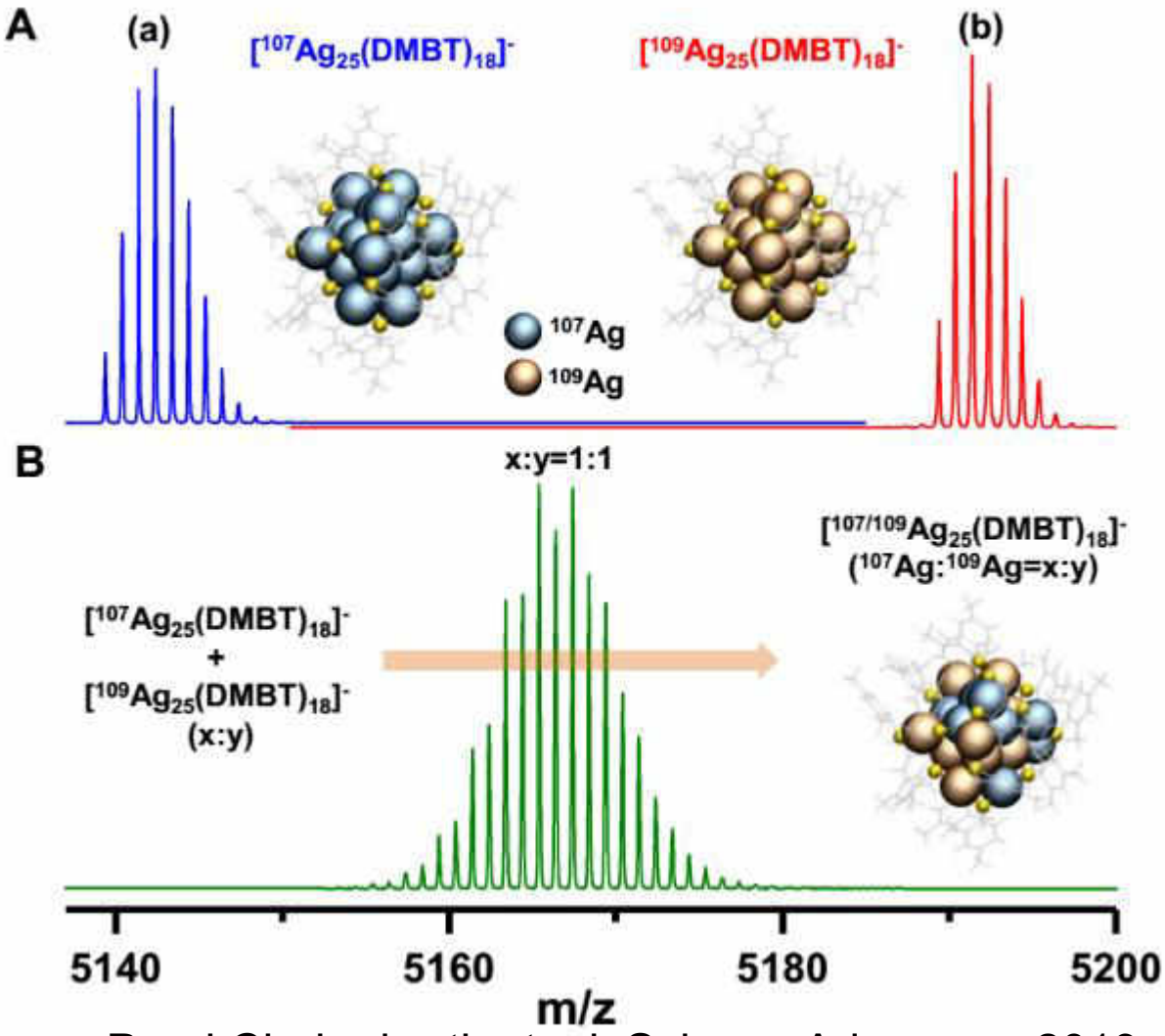

Papri Chakraborti, et. al. Science Advances, 2019.

New Clusters and new Ligands

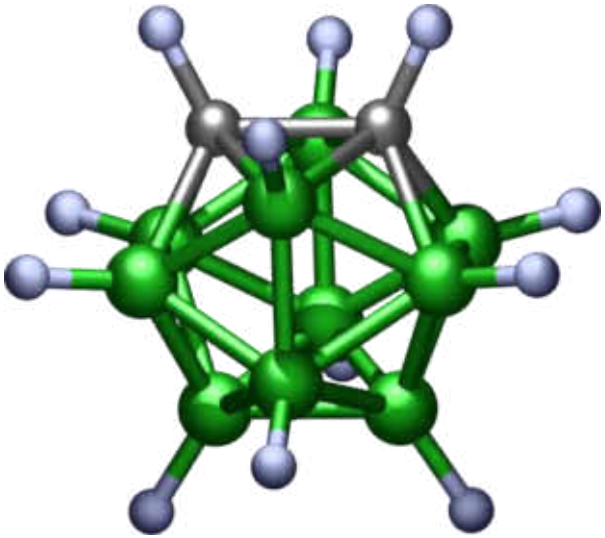

1,2-$C_2B_{10}H_{12}$

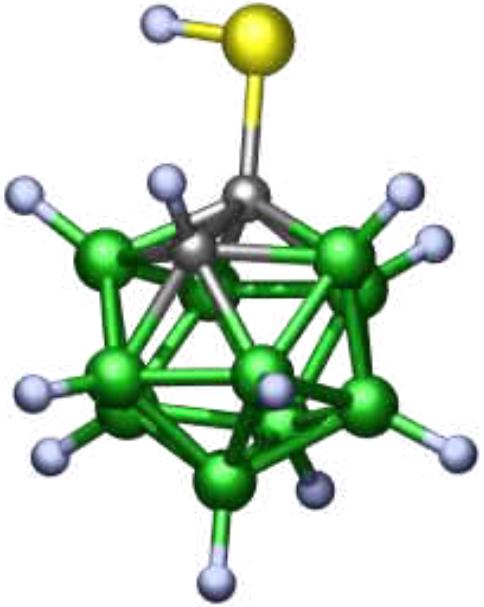

1-HS-1,2-$C_2B_{10}H_{11}$

Vivek Yadav, et. al., *Nature Communications*, Revised and submitted

Clusters stable up to 300 ºC!

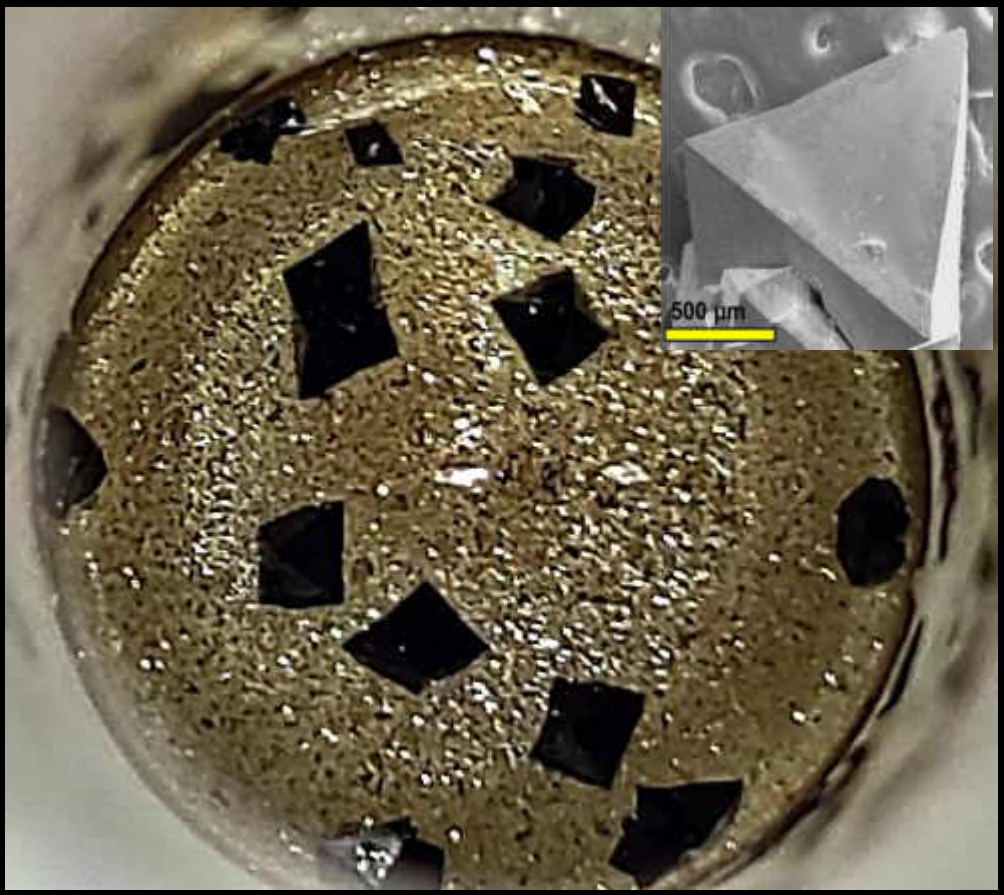

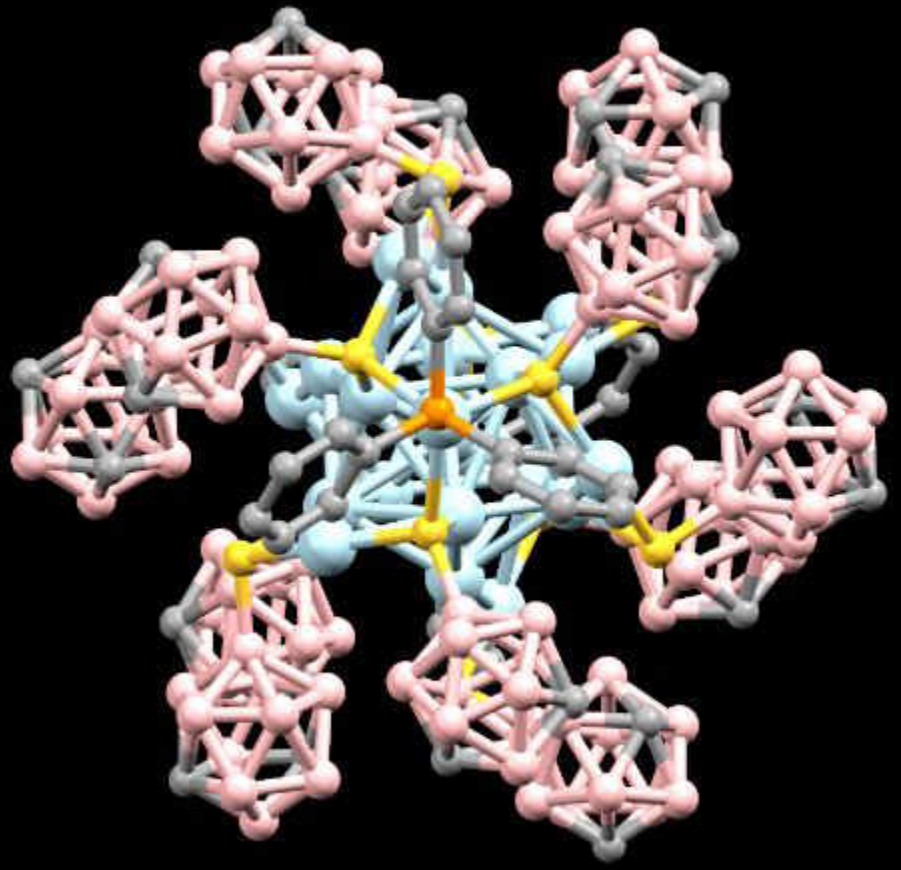

With Tomas Base

Jana *et. al*, Inorganic Chemistry (2022)

Structure of $[Ag_{17}(o_1\text{-}CBT)_{12}]^{3-}$ Nanocluster

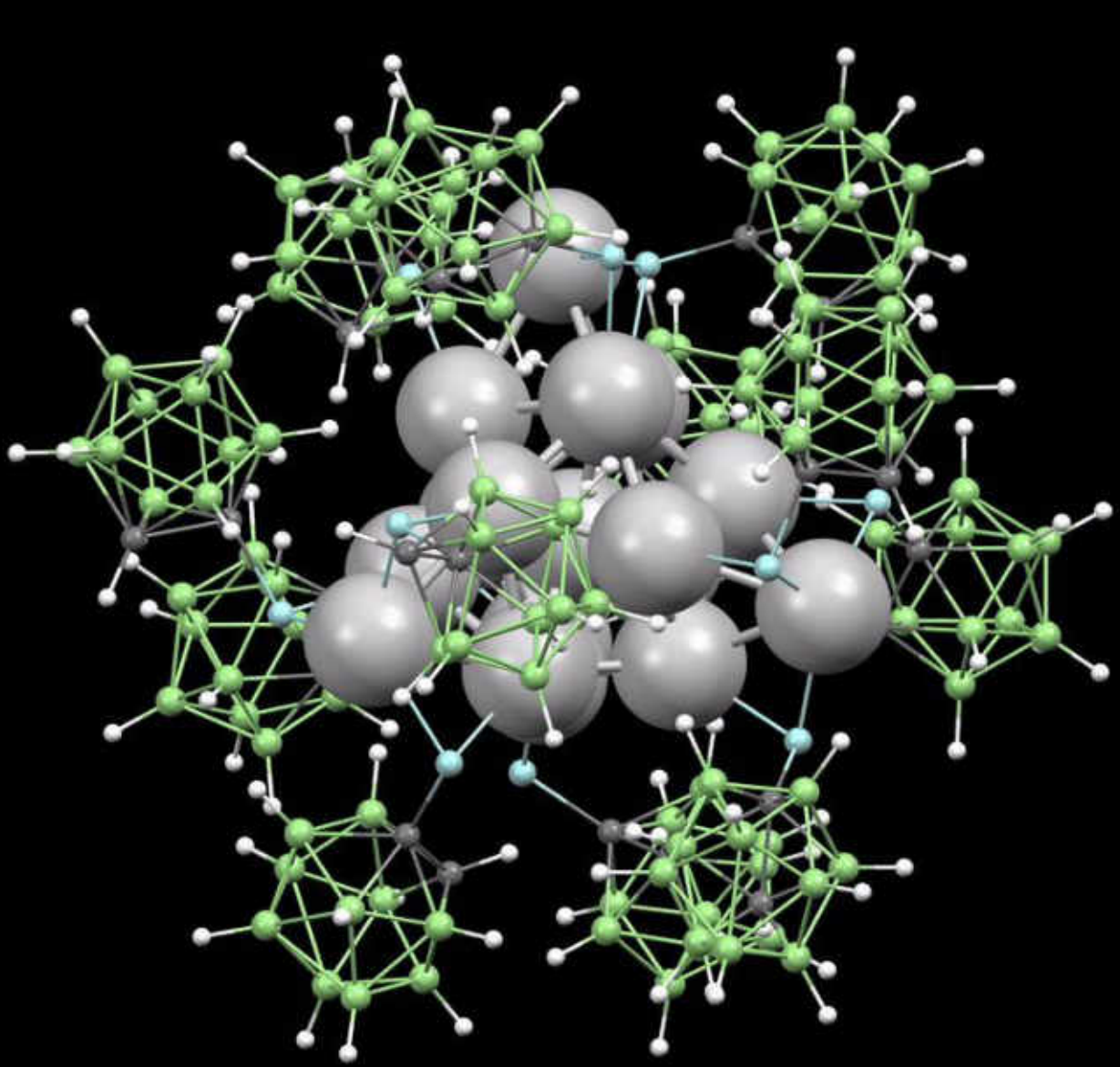

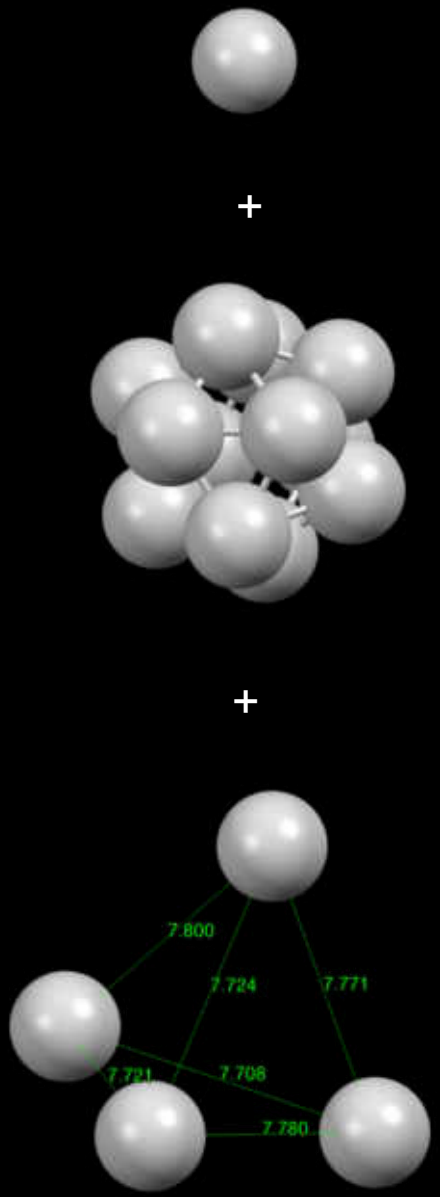

Structure of M_{17} Nanoclusters

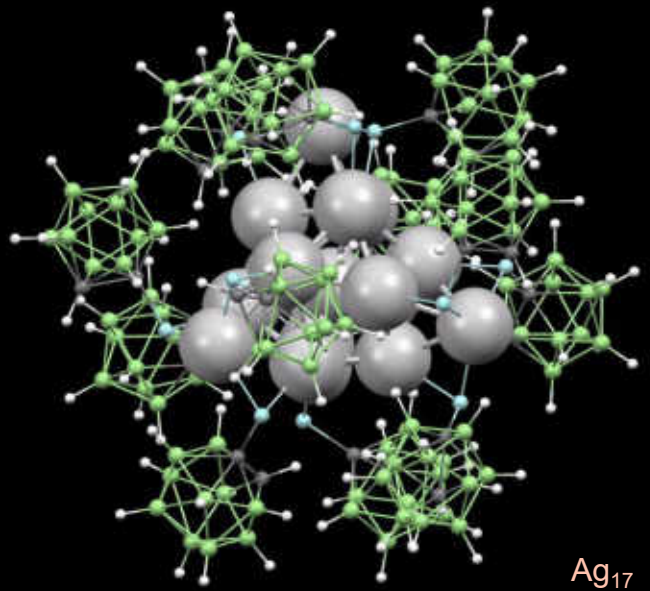

Ag_{17}

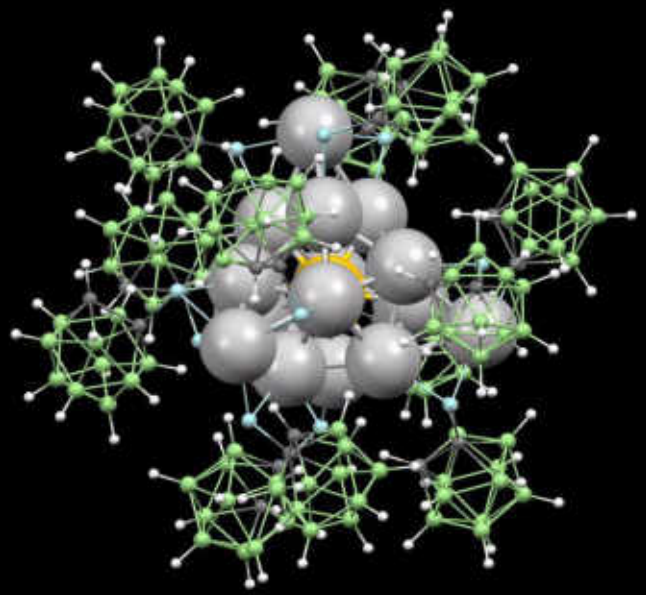

$Au@Ag_{16}$

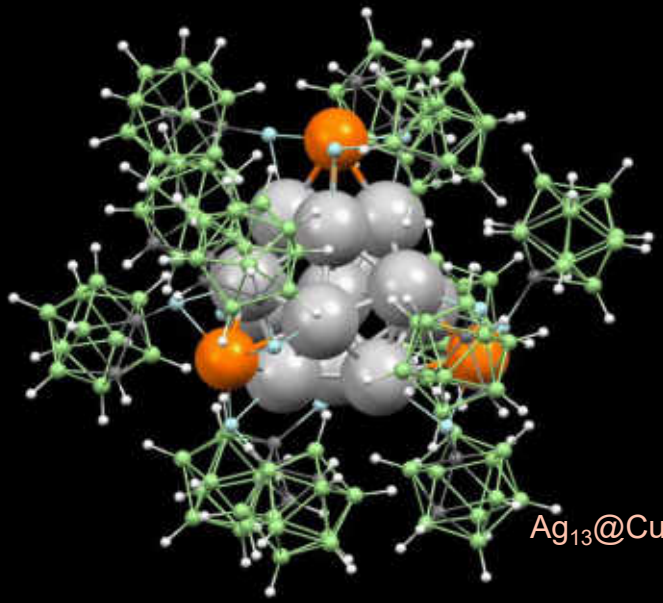

$Ag_{13}@Cu_4$

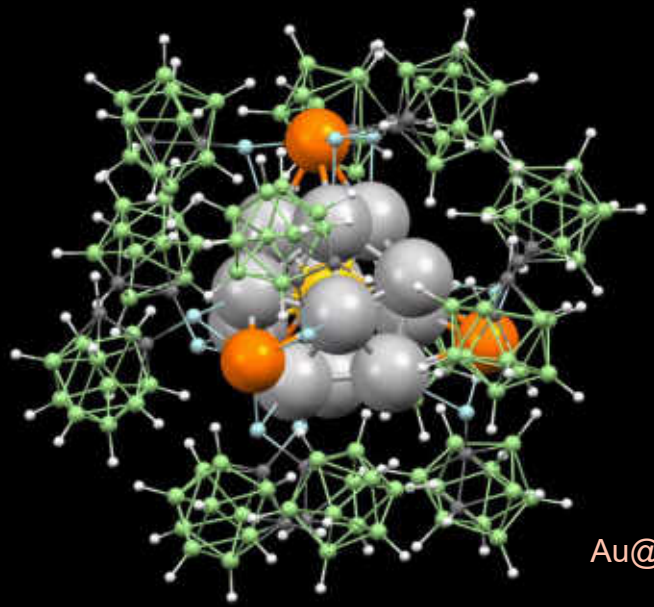

$Au@Ag_{12}@Cu_4$

Atomically precise nanocluster assemblies encapsulating plasmonic gold nanorods

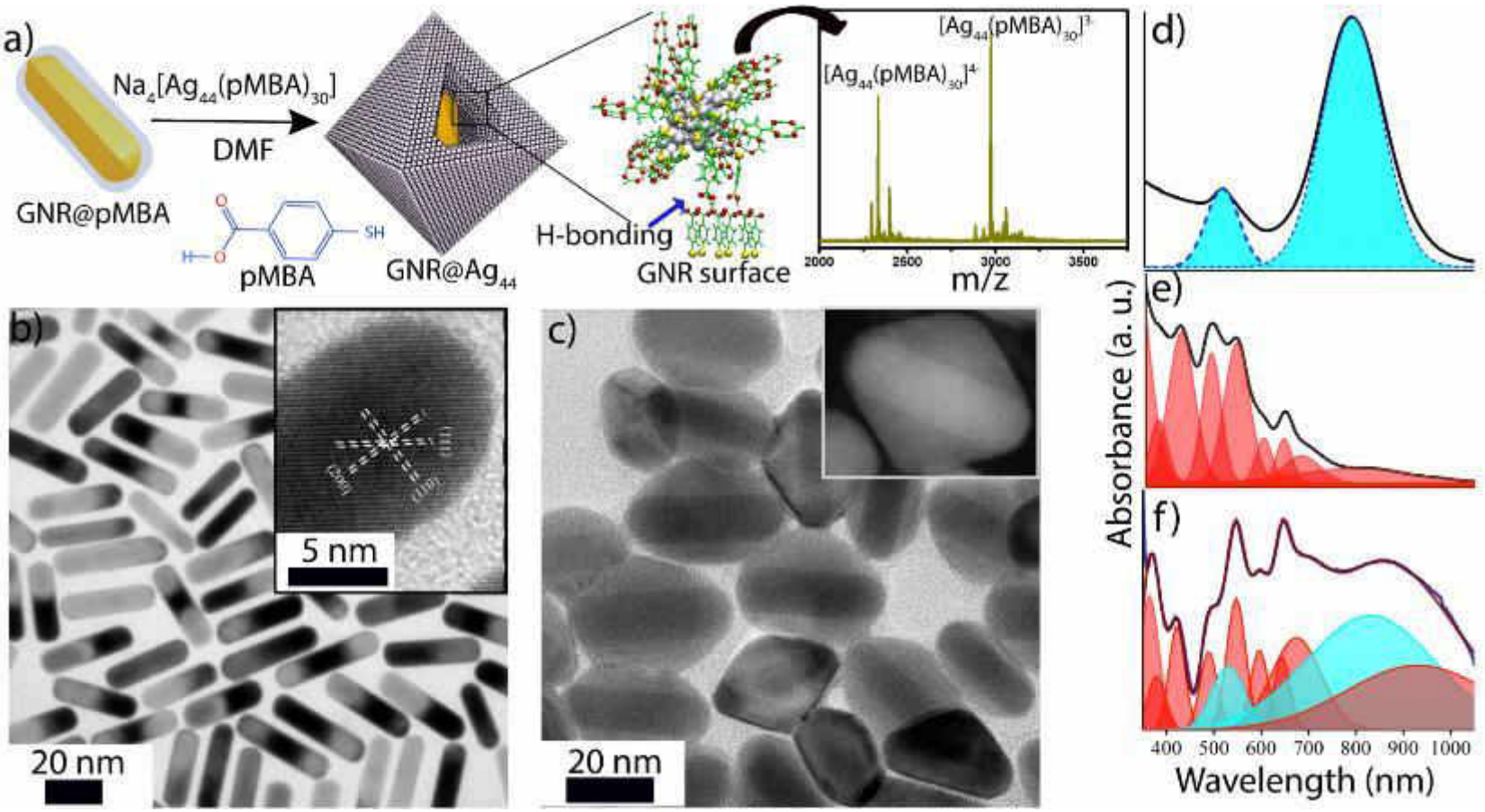

Chakraborty, A. et al., Angew. Chem. Int. Ed. **2018,** 57, 6522–6526.

A system of nomenclature

Aspicules

Gana Natarajan, et. al. JPC C. 2023

Ball and stick structure

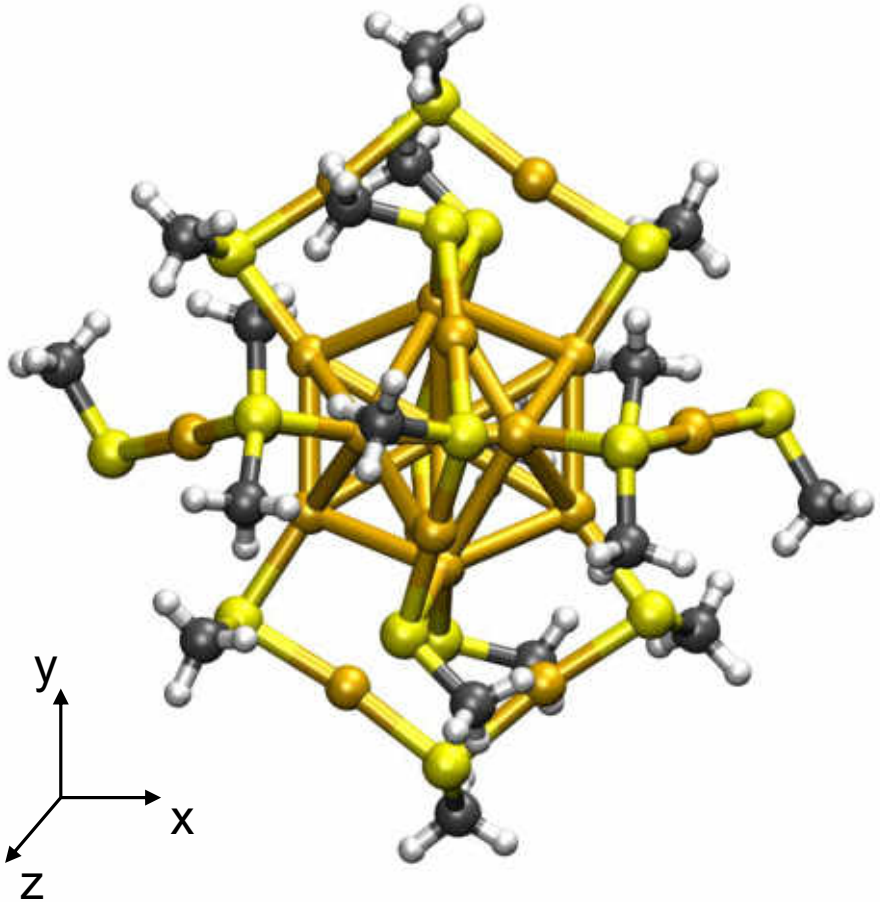

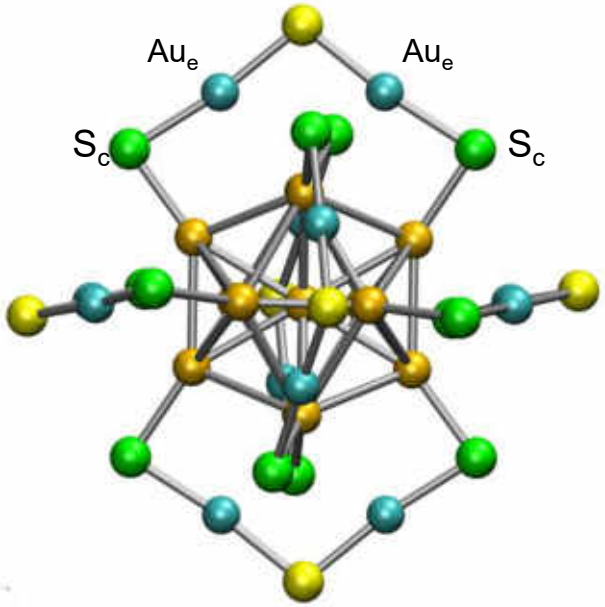

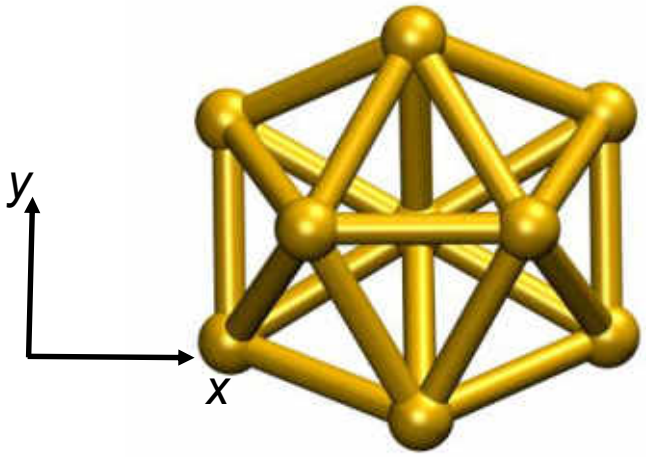

A view of gold methly thiolate [25]aspicule ($Au_{25}(SMe)_{18}$). Gold atoms colored gold, sulfur atoms by yellow, carbon dark gray, hydrogen atoms as white and (b) with the gold and sulfur atoms alone .

Shell Structure

(a) $Au@Au_{12}@Au_{12}@S_6@S_{12}$

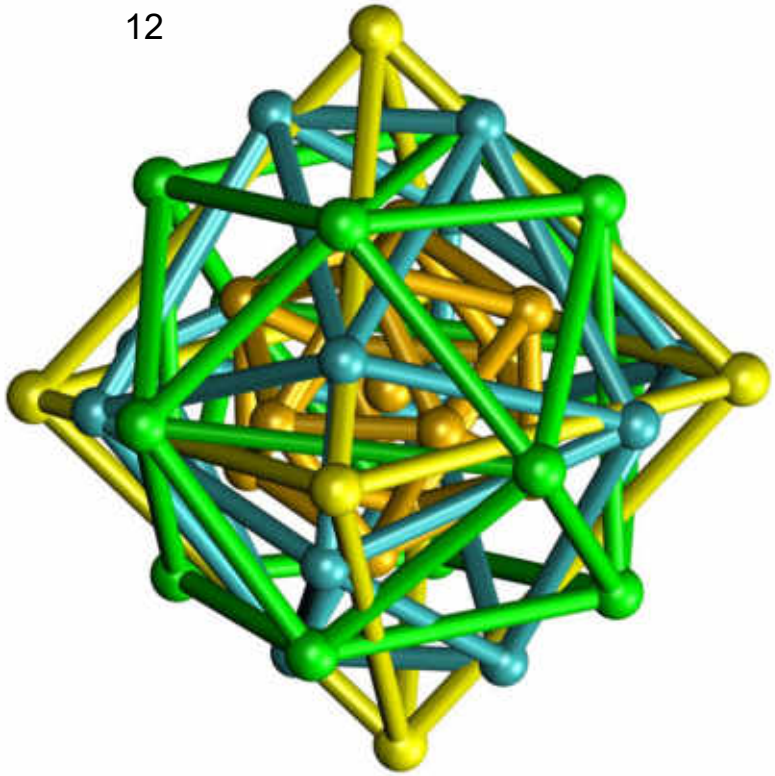

(b) $Au_{12}@Au_{12}$

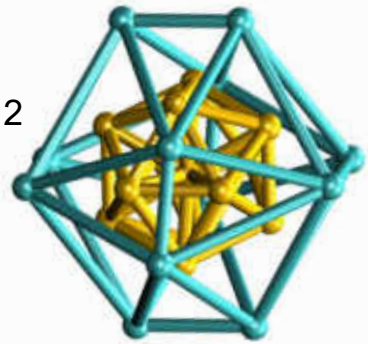

(c) $S_{12}@S_6$

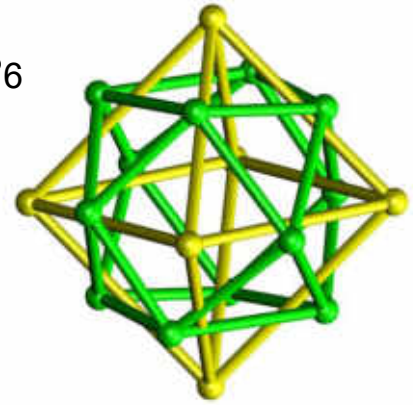

Terminologies

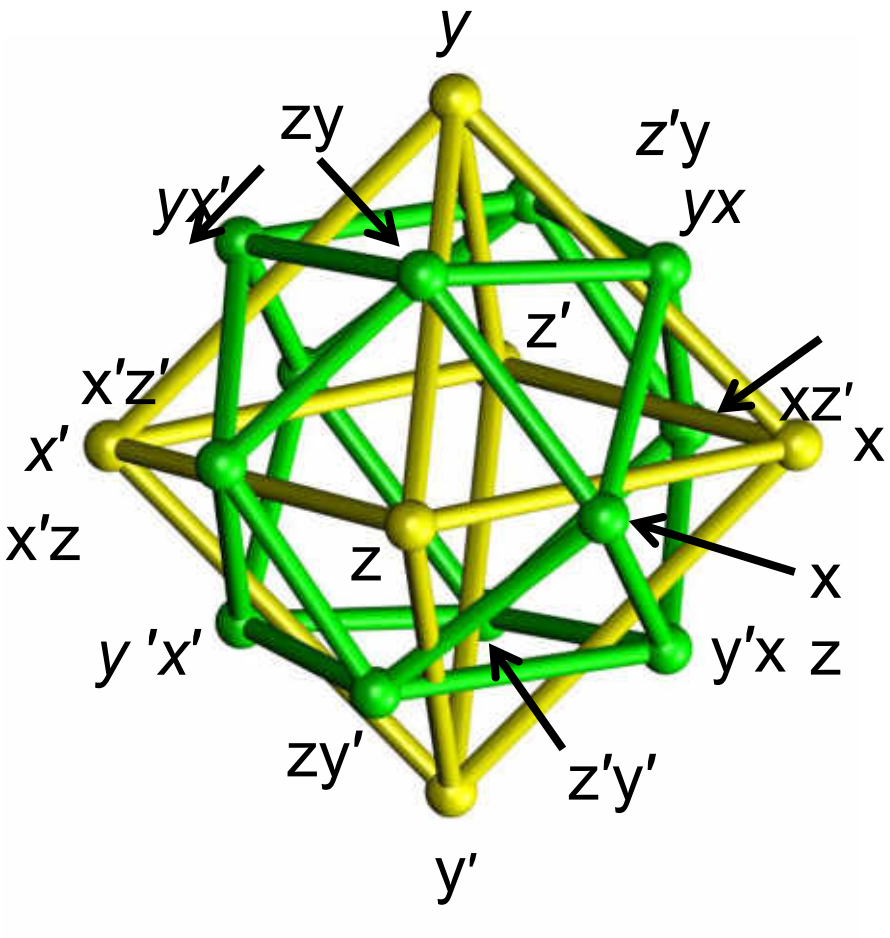

1) Edge projection

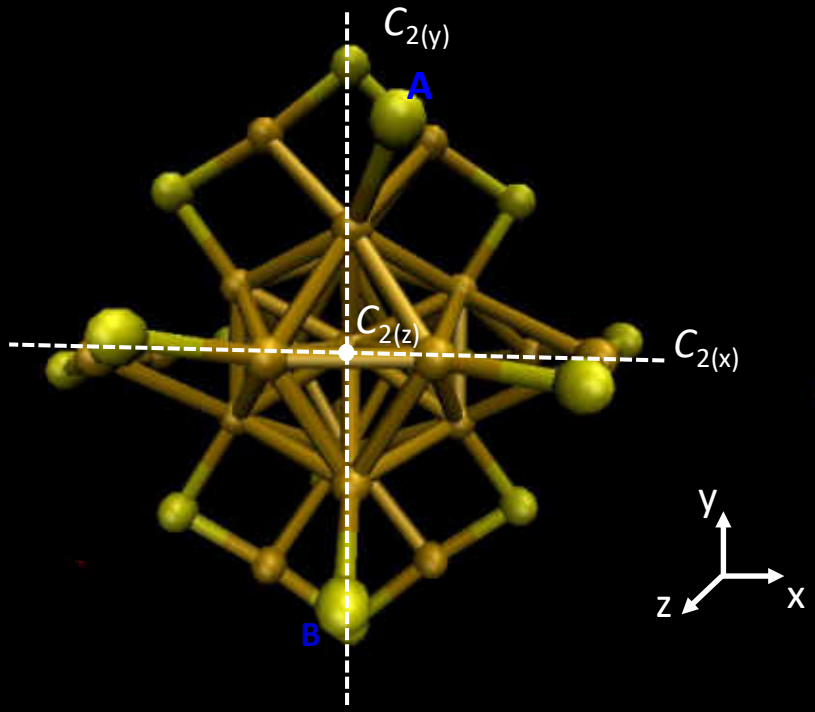

2) Face Projection

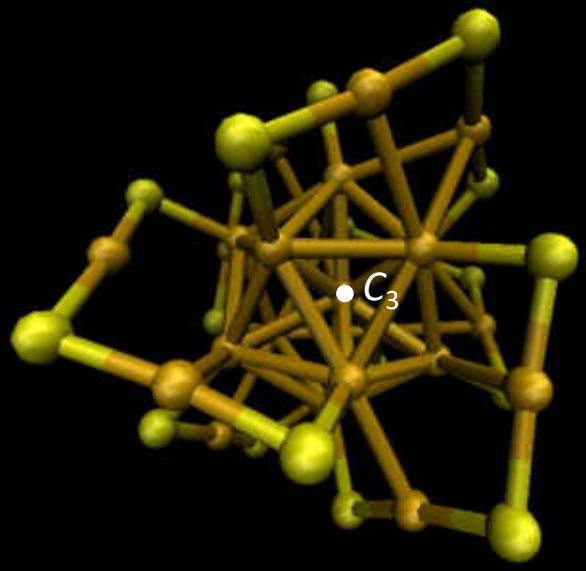

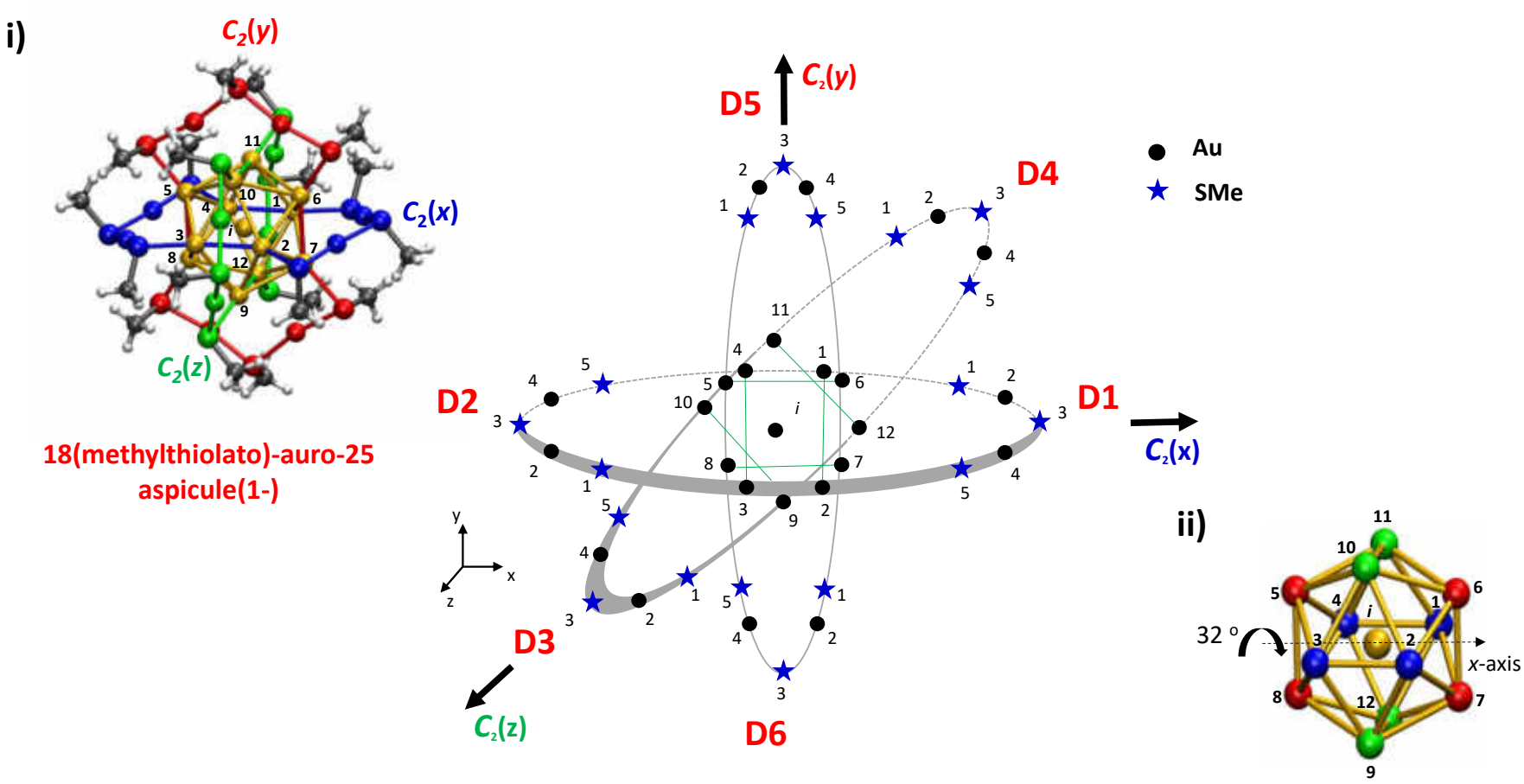

18(methylthiolato)-auro-25 aspicule(1-)

(D1-3,D2-3)-di(2-phenylethylthiolato),16(methylthiolato)-auro-25 aspicule(1-)
(D1-3,D2-3)-$(PET)_2$,$(SMe)_{16}$-auro-25 aspicule(1-)

Ligand Exchange & Alloy cluster

$Au_{24}Pd(SR_1)_{10}(SR_2)_8$ isomer 1 (cis)

1, 5-$(SBB)_{10}$, 3-$(SC_6H_{12})_8$
(i, 1, 2, x2)-palladoauro-25 asp (-1)

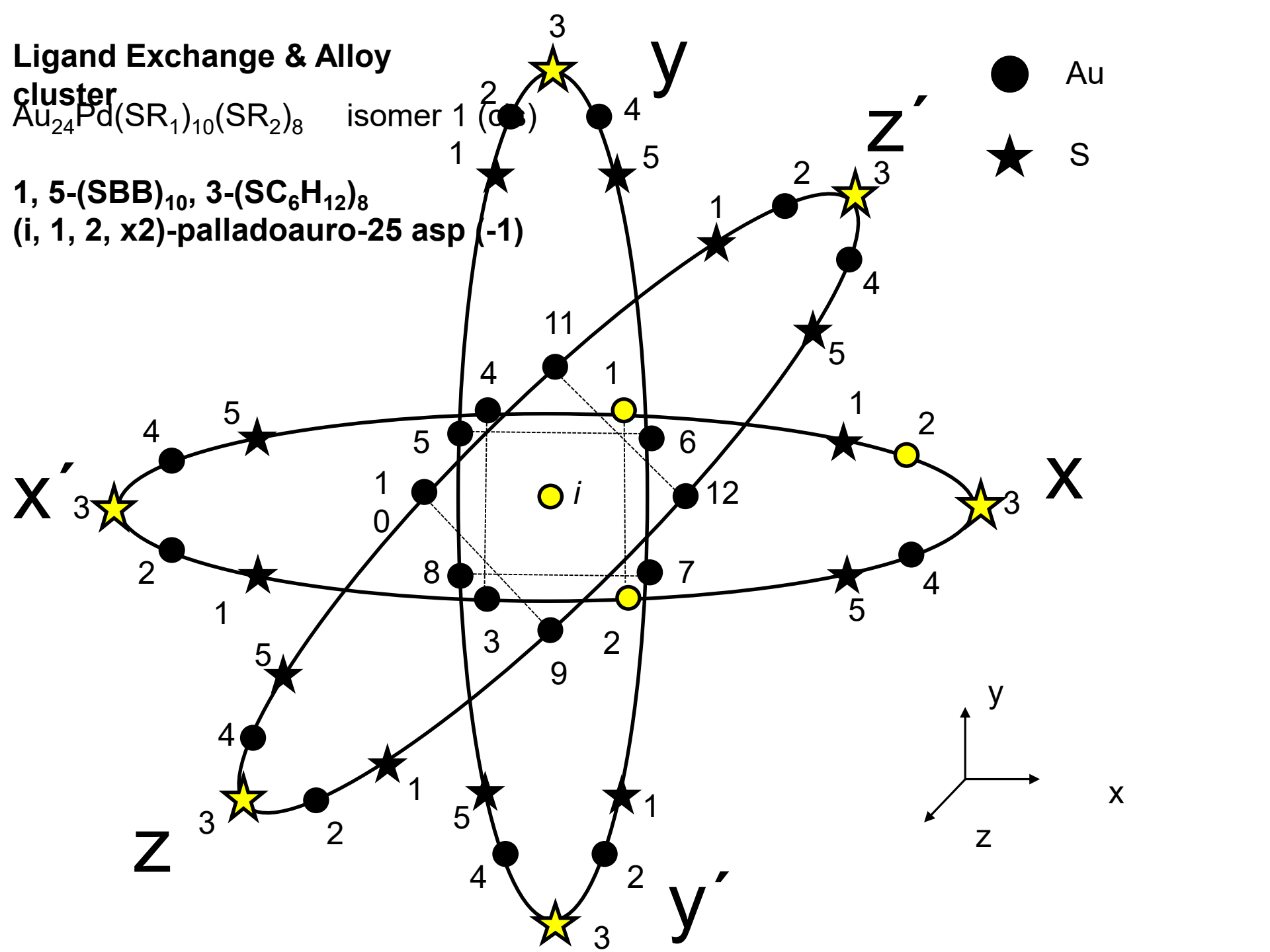

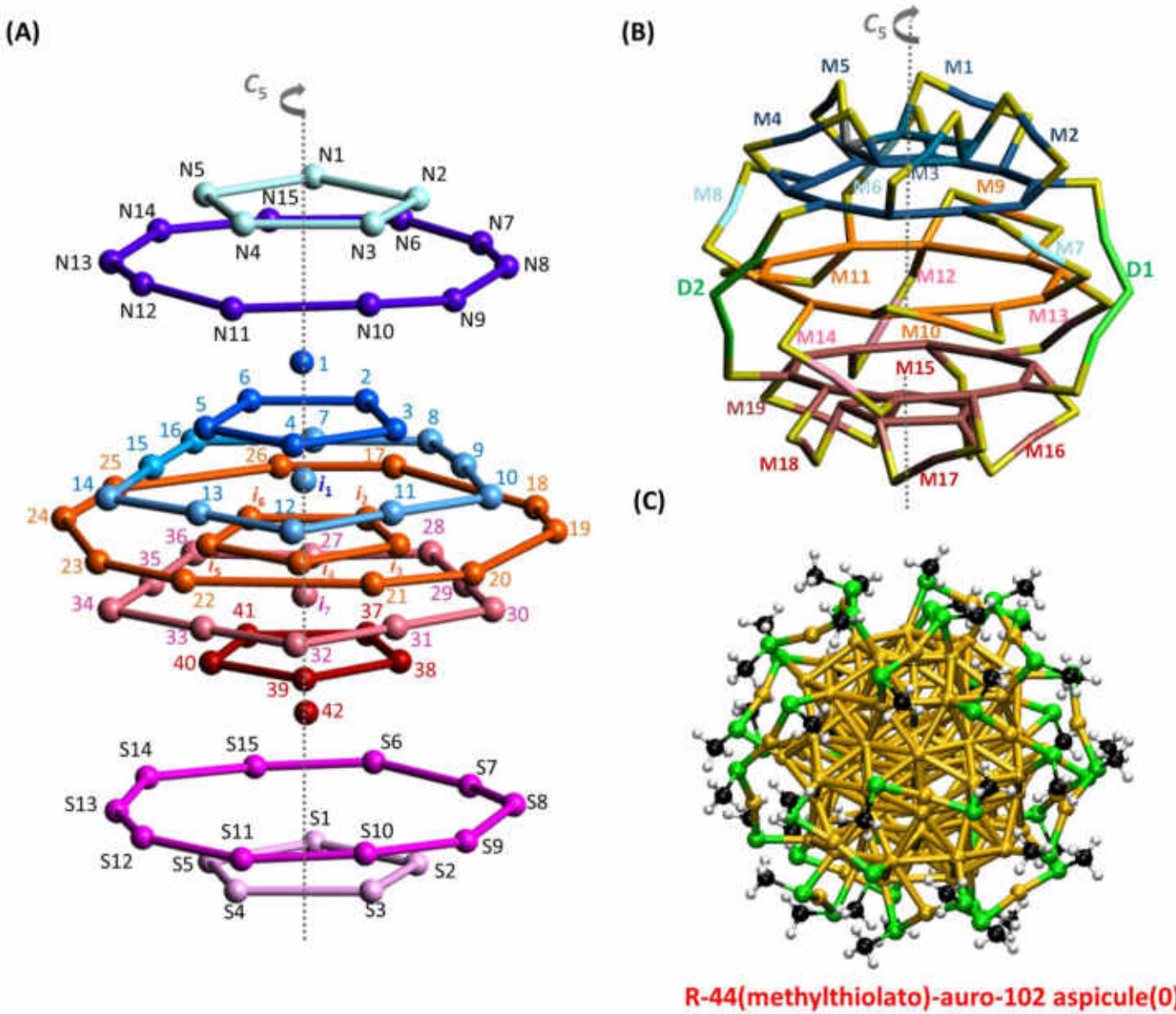

R-$(SMe)_{44}$-auro-102 aspicule**(**0**)** and L-$(SMe)_{44}$-auro-102 aspicule**(**0**)**

PNAS PNAS PNAS

Biopolymer-re nanocomposit water purifica

Mohan Udhaya Sankar[1], Saha Kamalesh Chaudhari, and Tha

Unit of Nanoscience and Thematic Uni

Edited by Eric Hoek, University of Calif

Creation of affordable materials fo water is one of the most promising drinking water for all. Combinin composites to scavenge toxic sp other contaminants along with th affordable, all-inclusive drinking v without electricity. The critical p synthesis of stable materials tha uously in the presence of comp drinking water that deposit and surfaces. Here we show that suc be synthesized in a simple and effe out the use of electrical power. T sand-like properties, such as highe forms. These materials have beer water purifier to deliver clean drin ily. The ability to prepare nanos ambient temperature has wide water purification.

hybrid | green | appropriate technolog

Work was featured in several journals

Nature Nanotechnology, July 2014 issue

We developed environmentally friendly water positive nanoscale materials for affordable, sustainable and rapid removal of arsenic from drinking water.

There are over 1700 community installations across the country, serving 1.3 million people with arsenic and iron-free water every day.

Quantum cluster based metal ion sensing paper

Large area uniform illumination using quantum cluster

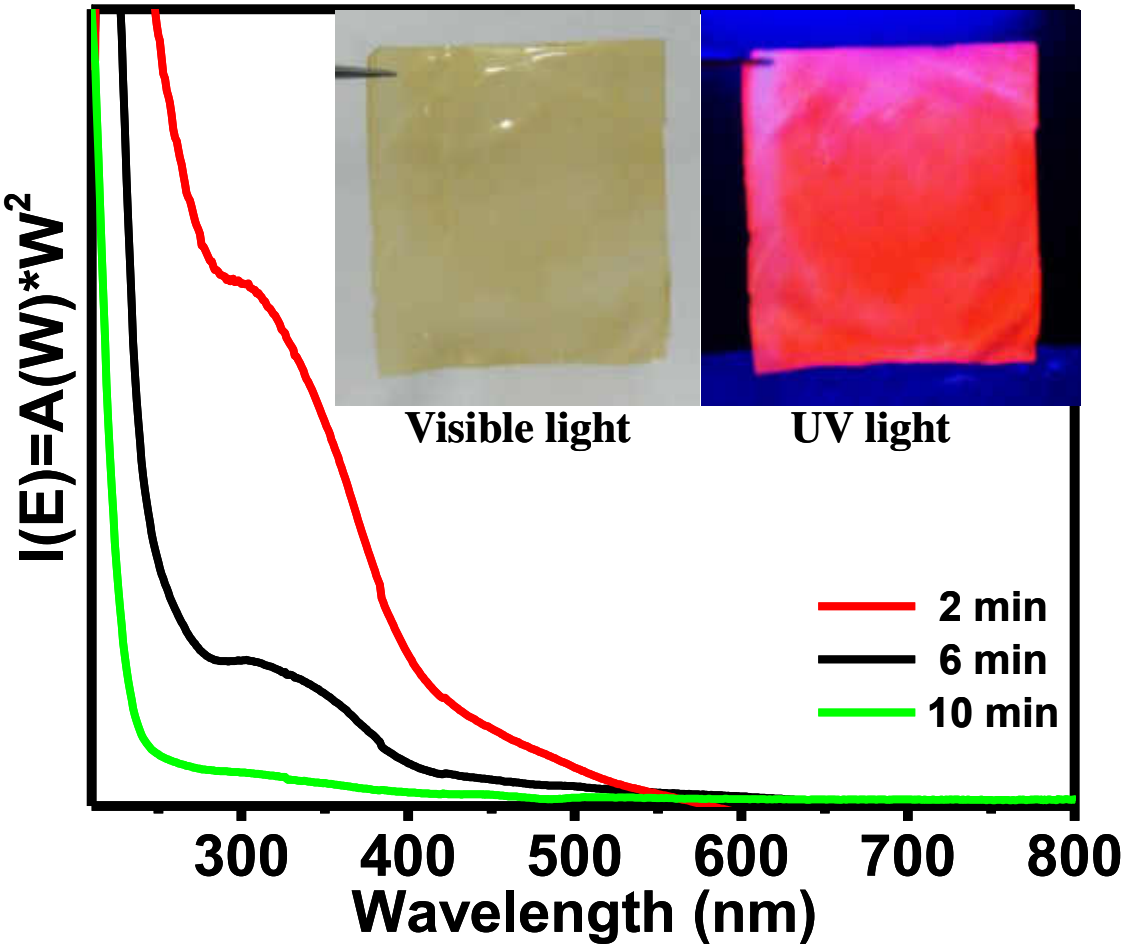

Decrease in the absorption of Au_{15} as a biofilm is dipped into the cluster solution. Inset: Free standing quantum cluster loaded film in visible light and UV light.

Anu George et al. *ACS Applied Materials & Interfaces*, 2012

Approaching detection limits of tens of Hg^{2+}

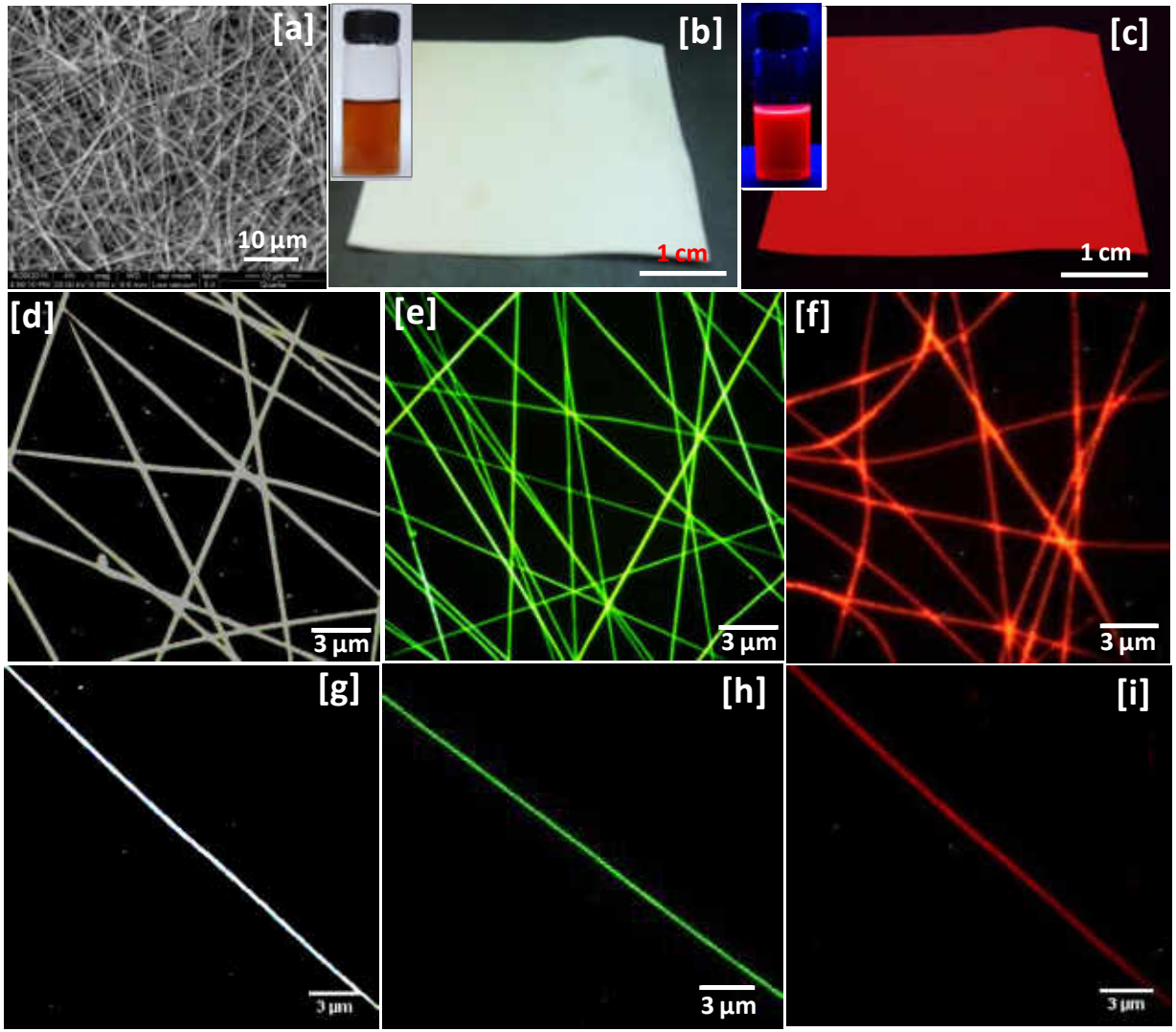

Atanu Ghosh et al. Anal. Chem.2014.

Video of mercury quenching experiment using the nanofiber

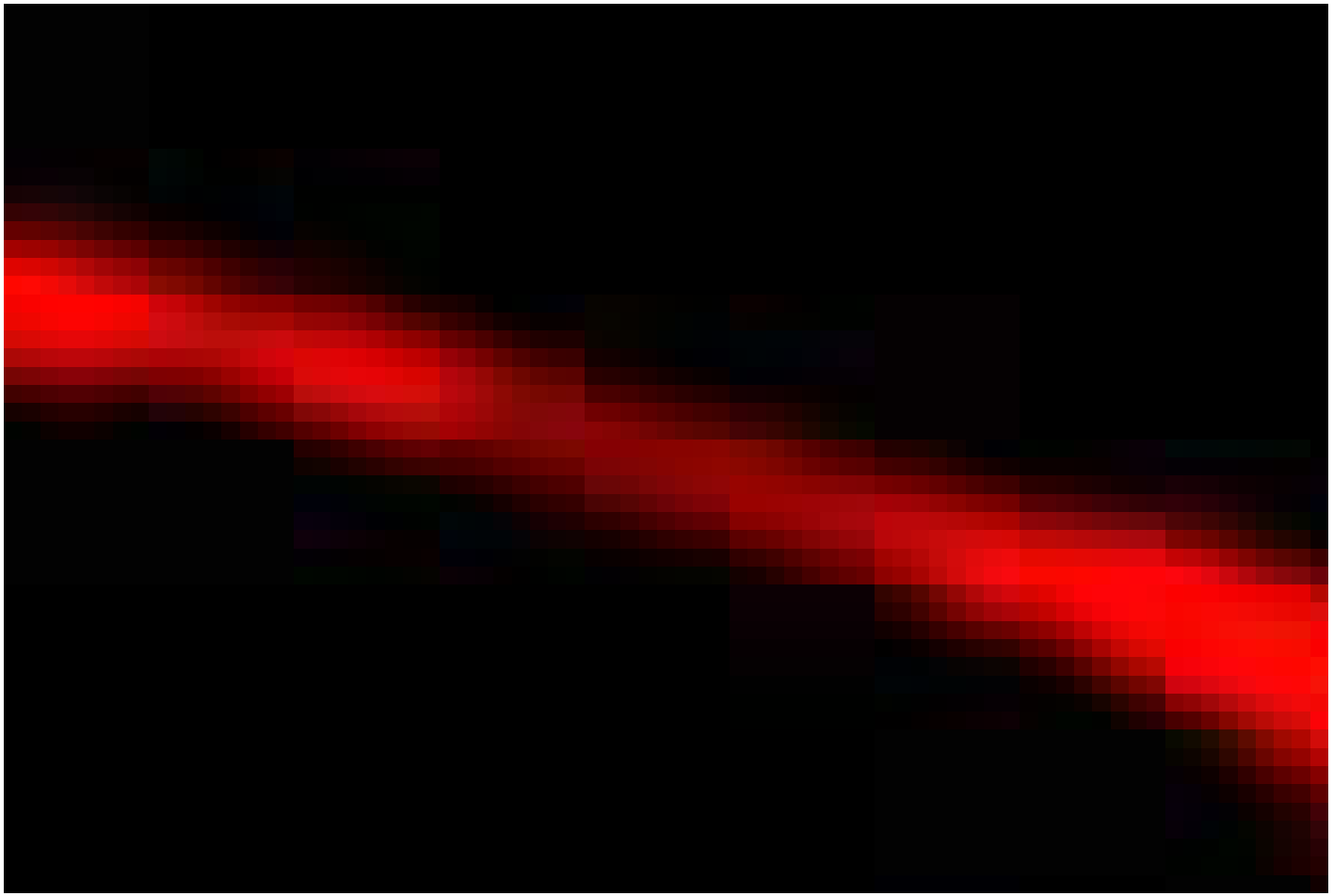

Sensors and new opportunities

Analog/Grating
Equipment
$ 5~6 Billion (2017)
a few **100k units (2017)**

Ultra compact Low Cost
Spectral Sensor Module
~ Billions units (? 2027)

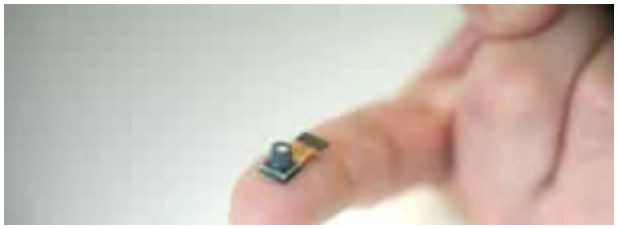

Water quality measurement – In the pipeline

nanoλ

New electrodes - Aligned nanoplates of Co_6S_8

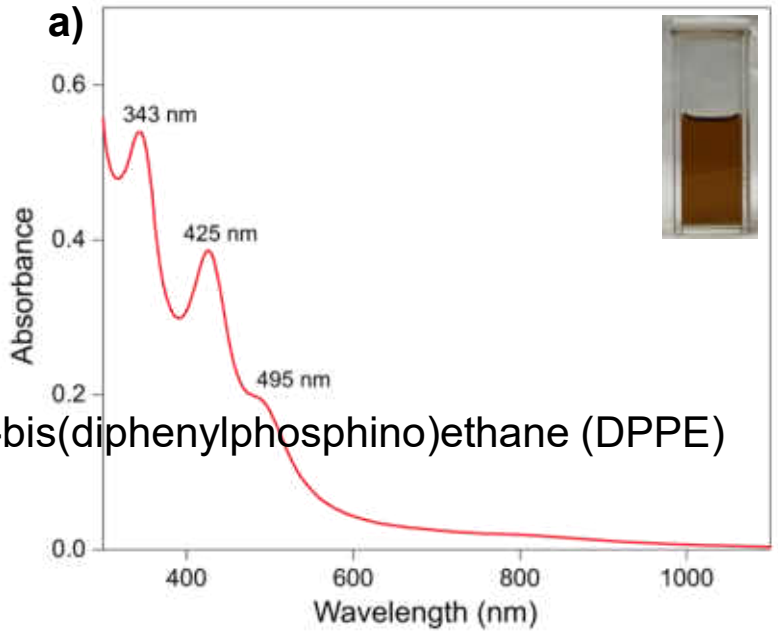

1,2-bis(diphenylphosphino)ethane (DPPE)

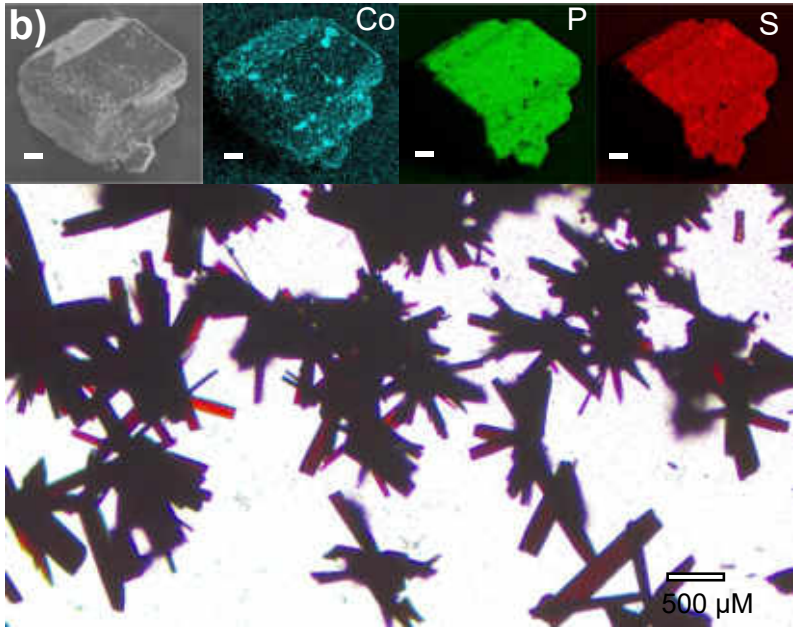

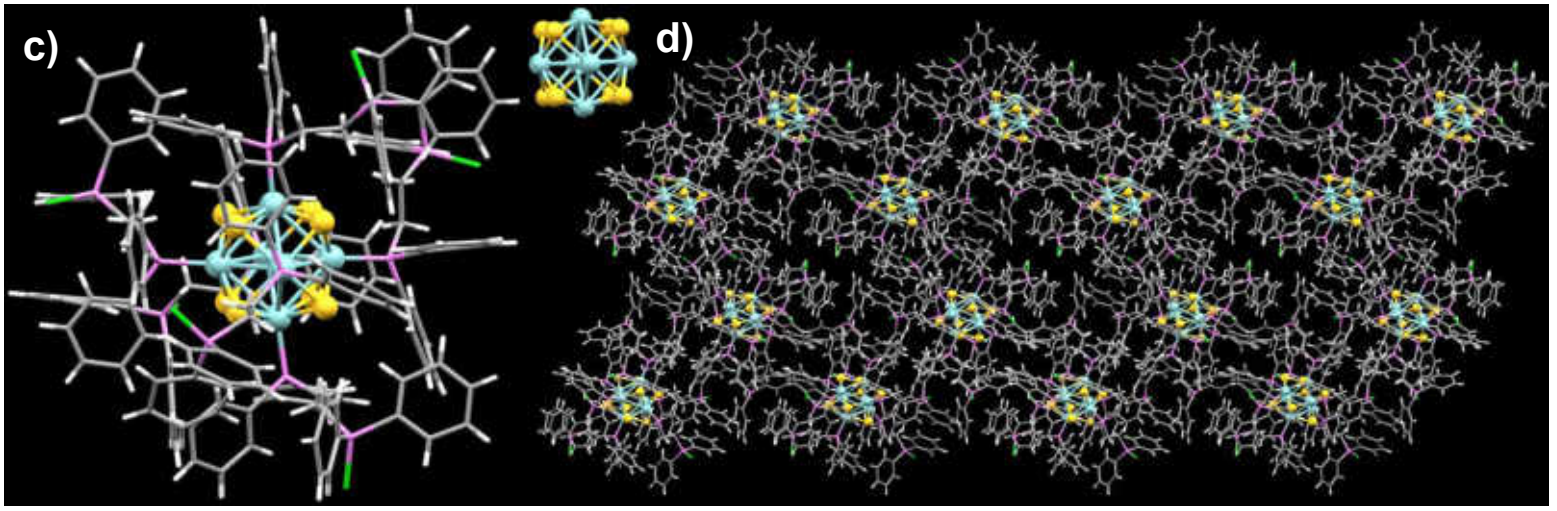

Electrospray deposition

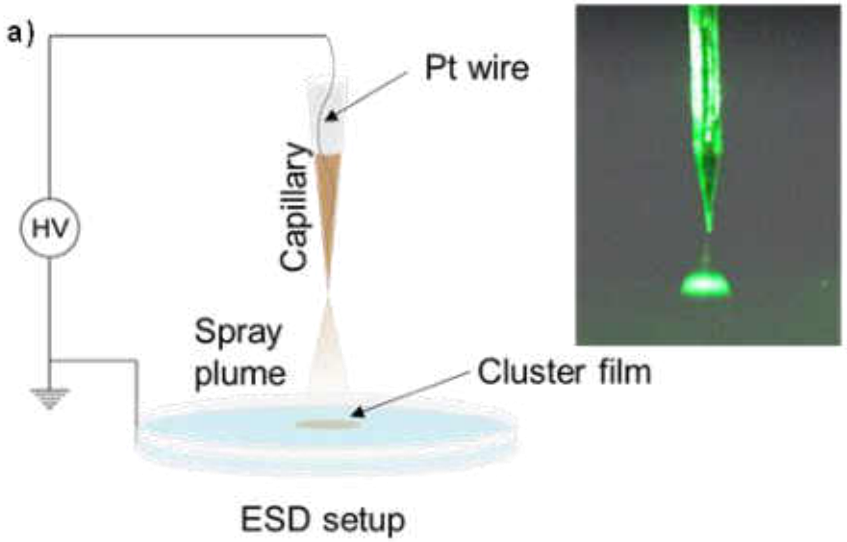

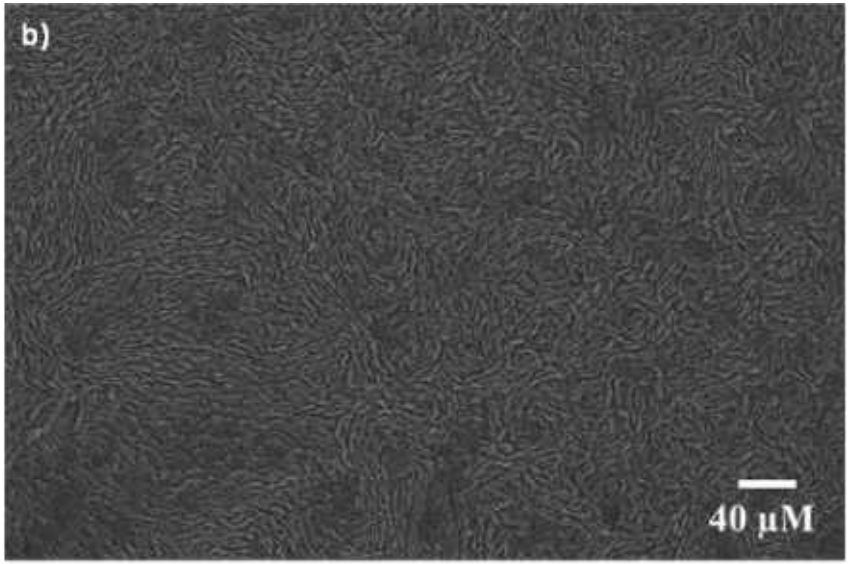

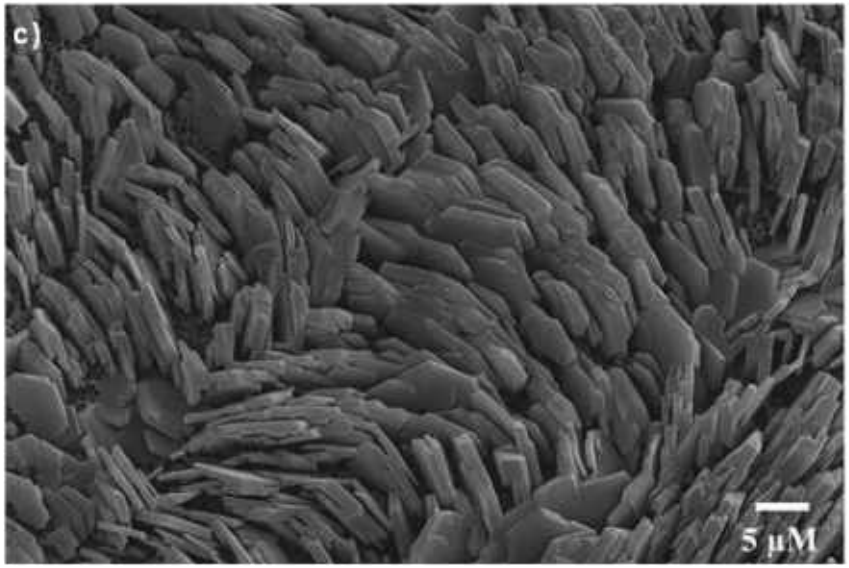

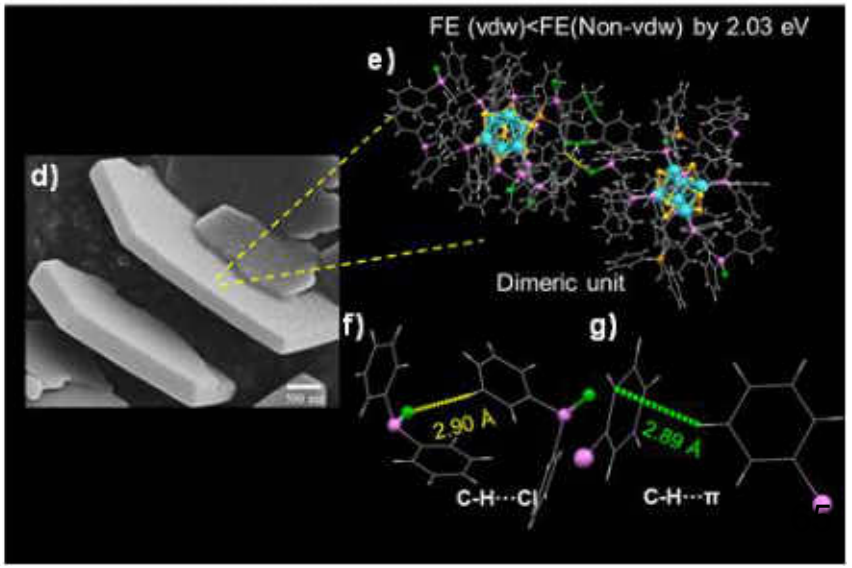

Sensing

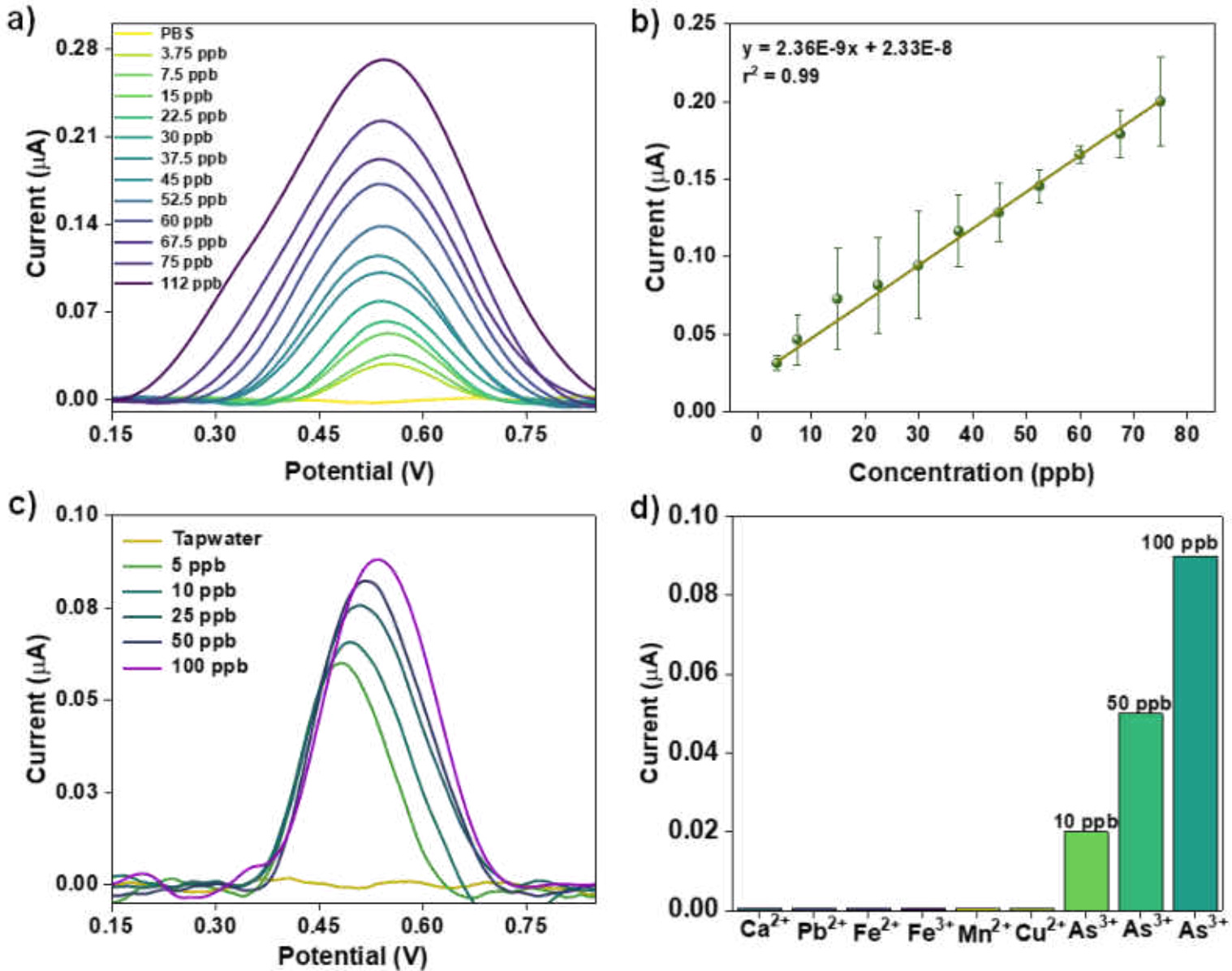
a)
PBS
3.75 ppb
7.5 ppb
15 ppb
22.5 ppb
30 ppb
37.5 ppb
45 ppb
52.5 ppb
60 ppb
67.5 ppb
75 ppb
112 ppb
Current (μA)
Potential (V)
b)
y = 2.36E-9x + 2.33E-8
r² = 0.99
Current (μA)
Concentration (ppb)
c)
Tapwater
5 ppb
10 ppb
25 ppb
50 ppb
100 ppb
Current (μA)
Potential (V)
d)
100 ppb
50 ppb
10 ppb
Current (μA)
Ca2+ Pb2+ Fe2+ Fe3+ Mn2+ Cu2+ As3+ As3+ As3+

Working electrode

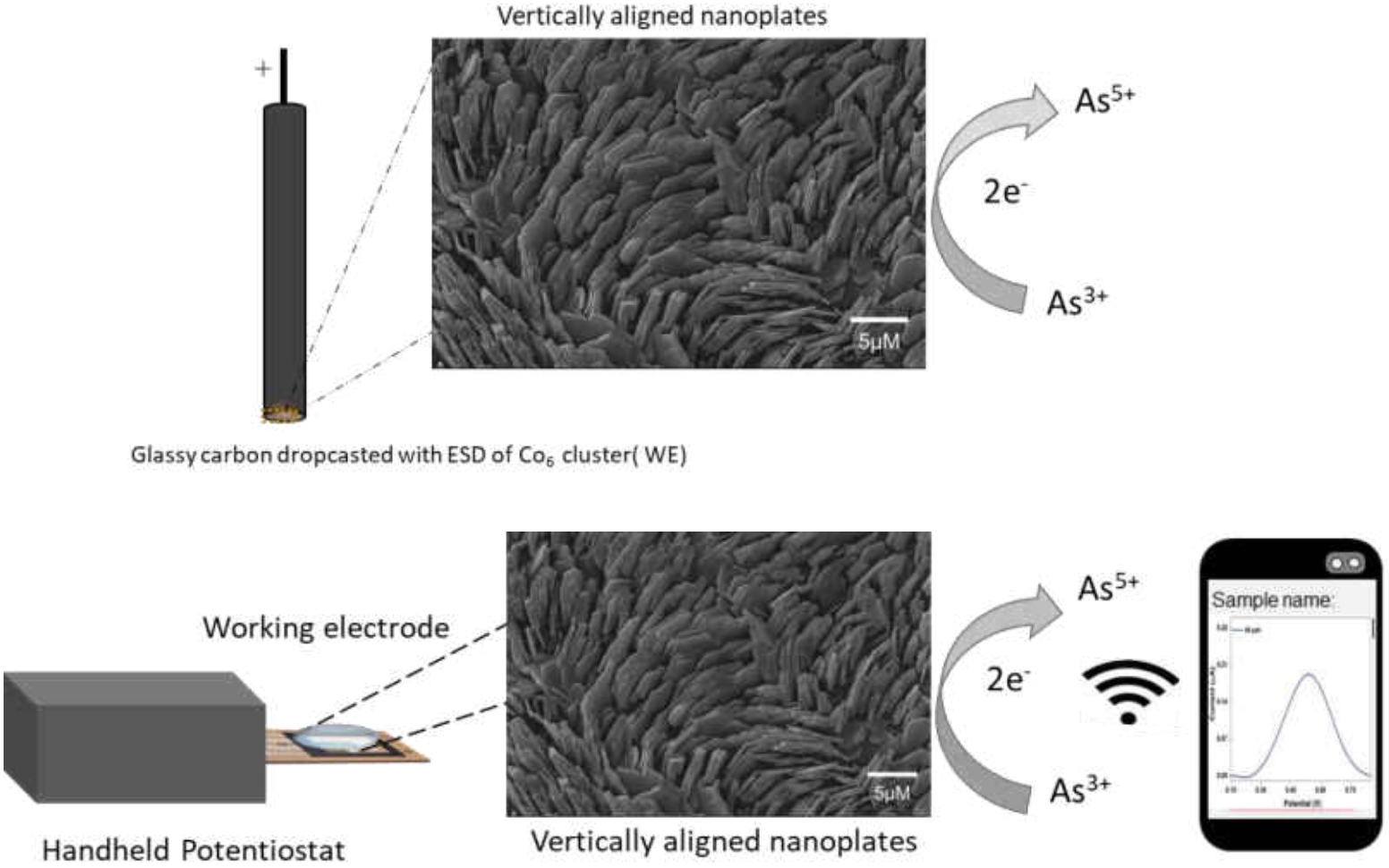

Anagha Jose et al. *ACS Materials Lett.,* 5 (2023) 893–899.

Arsenic poisoning across the world

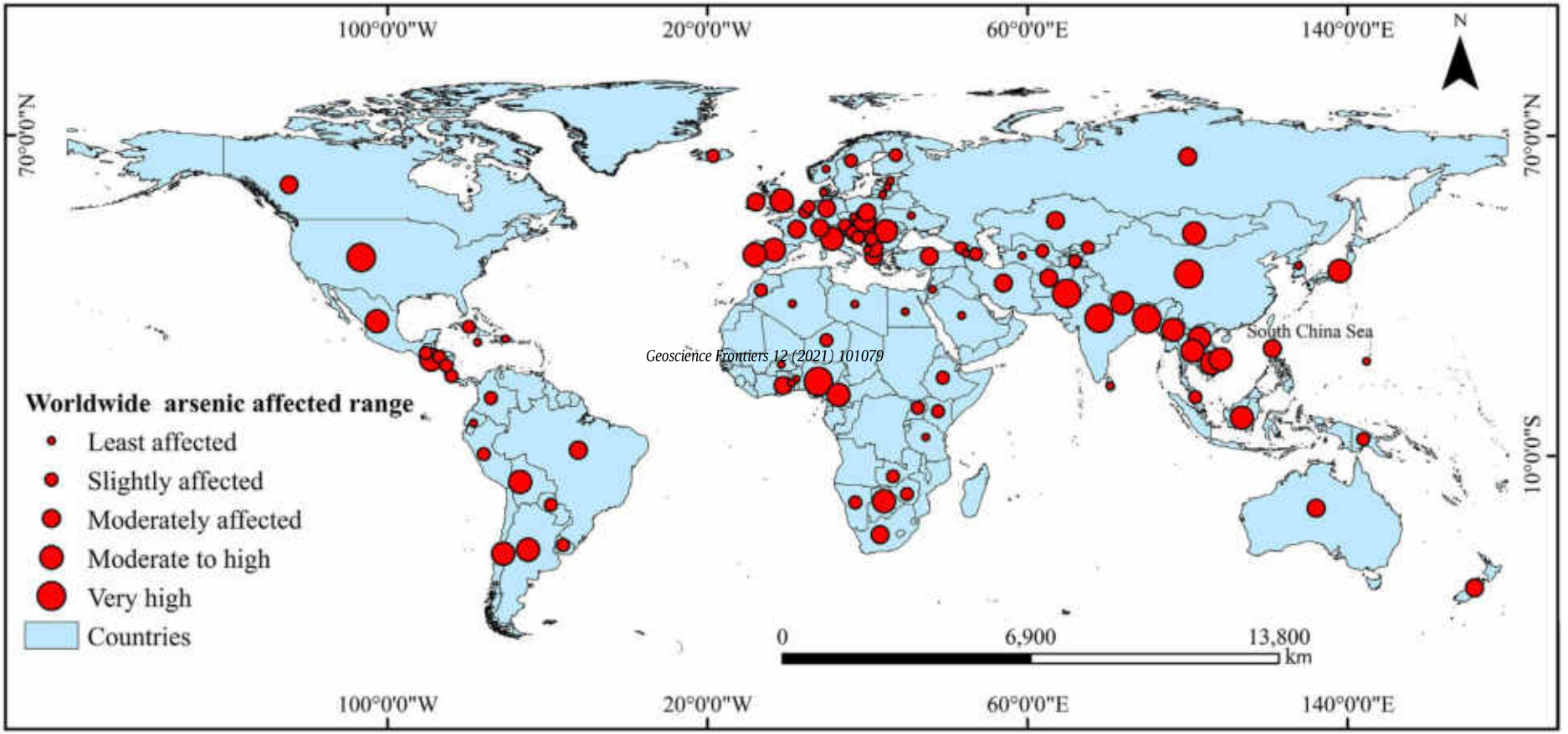

E. Shaji, M. Santosh, K. V. Sarath, Pranav Prakash, V. Deepch and B. V. Divya, Geoscience Frontiers, 12 (2021) 101079.

India’s water is being monitored

IITM/IISc

Installations made by four companies

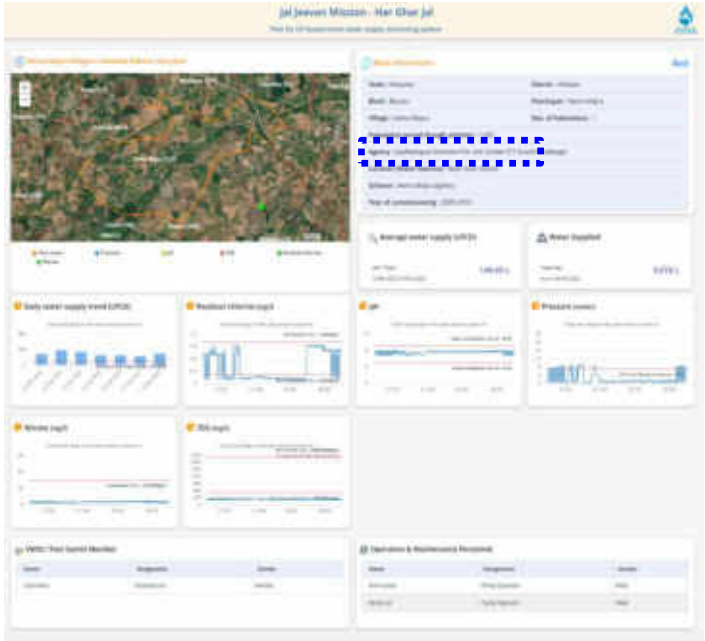


International Centre for Clean Water


IIT Madras Research Park

Collaborators






Tatsuya Tsukuda
Keisaku Kimura
Yuichi Negishi
Hannu Hakkinen
Uzi Landman
Rob Whetten
K. Vijayamohanan, Reji Philip, Shiv Khanna

Robin Ras

Nonappa

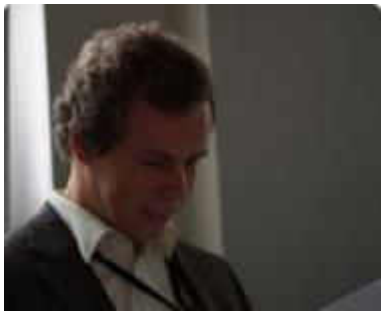

Tomas Base

Manfred Kappes

Olli Ikkala

Horst Hahn

Biswarup Pathak

K. V. Adarsh

G. U. Kulkarni

Vivek Polshettiwar

Indian Institute of Technology Madras

Bhaskar Ramamurthi/V. Kamakoti

Associate Editor

ACS Sustainable Chemistry & Engineering